Supplementary Information

Halide-free pyridinium base binary organocatalyst for the cycloaddition of carbon dioxide with epoxides

Xin Yuan[a], Ziqi Liu[a], Zhenjiang Li[a,*], Yanqi Shi[a], Baolin Yang[a], Xin Zou[a], Yongzhu Hu[a], Chunyu Li[a], Sha Li[b], and Kai Guo[a,*]

[a] *State Key Laboratory Materials-Oriented Chemical Engineering, College of Biotechnology and Pharmaceutical Engineering, Nanjing Tech University, 30 Puzhu Road South, Nanjing 211816, China.*

[b] *College of Food Science and Light Industry, Nanjing Tech University, 30 Puzhu Road South, Nanjing 211816, P. R. China.*

** Corresponding authors.*

E-mail: guok@njtech.edu.cn (K. Guo); zjli@njtech.edu.cn (Z. Li)

Table of Contents

1. General information

Materials. CO_2 was supplied by Nanjing Shangyuan Industrial Gas Factory with a purity of 99.99%. Epoxides were purchased from Alfa Aesar. Organic base and hydroxy pyridine with different substituents were supplied by Sinopharm Chemical Reagent Co. All the other reagents were purchased from Aldrich and used without further purification.

Characterizations. ^{1}H and ^{13}C NMR spectra were recorded on a Bruker Avance 400 and 101 MHz NMR spectrometer in $CDCl_3$, or DMSO-d_6 as stated deuterated solvents. Chemical shifts δ are reported in parts per million (ppm) relative to a residual undeuterated solvent as an internal reference (^{1}H δ 7.26 for $CDCl_3$, δ 2.50 for DMSO-d_6, ^{13}C δ 77.16 for $CDCl_3$, δ 39.52 for DMSO-d_6). Conversions and selectivity of epoxides were determined by ^{1}H NMR spectroscopy. All NMR experiments were performed at room temperature. Thermogravimetric analysis (TGA) was performed on a Mettler-Toledo TG50 and SDT Q600 TG-DTA analyser under N_2 atmosphere. Approximately 5 mg of polymer sample was weighed and equilibrated at 30 °C; Ramp 10 °C/min to 600 °C.

2. Spectral data of catalysts 1–12

1. TBD·*p*-HP

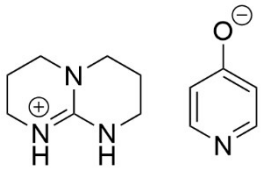

Yellow oil. **^{1}H NMR** (400 MHz, DMSO-d_6) δ 7.72 (d, J = 5.7 Hz, 2H), 6.69 (s, 2H), 6.10 (d, J = 5.7 Hz, 2H), 3.19 (d, J = 13.8 Hz, 8H), 1.85 (p, J = 5.9 Hz, 4H). **^{13}C NMR** (101 MHz, DMSO-d_6) δ 173.84, 151.04, 148.63, 115.59, 46.24, 37.57, 20.57.

2. TBD·*o*-HP

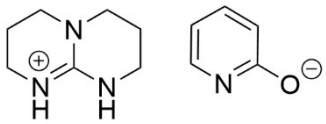

Yellow oil. **^{1}H NMR** (400 MHz, DMSO-d_6) δ 8.81 (s, 2H), 7.61 – 7.53 (m, 1H), 7.18 (ddd, J = 8.9, 6.9, 2.4 Hz, 1H), 6.08 – 5.99 (m, 2H), 3.26 – 3.17 (m, 8H), 1.85 (p, J = 5.9 Hz, 4H).

3. TBD·*m*-HP

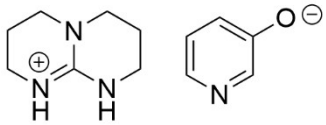

Yellow oil. **^{1}H NMR** (400 MHz, DMSO-d_6)δ 8.04 (s, 2H), 7.76 (d, J = 2.9 Hz, 1H), 7.48 (dd, J = 4.5, 1.4 Hz, 1H), 6.87 (dd, J = 8.2, 4.4 Hz, 1H), 6.66 (ddd, J = 8.3, 3.0, 1.5 Hz, 1H), 3.25 – 3.13 (m, 8H), 1.83 (p, J = 5.9 Hz, 4H).

4. MTBD·*p*-HP

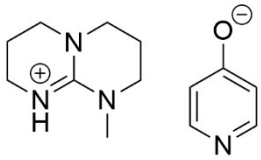

Yellow oil. **^{1}H NMR** (400 MHz, DMSO-d_6) δ 7.83 – 7.72 (m, 2H), 6.28 – 6.19 (m, 2H),

6.06 (s, 1H), 3.23 – 3.12 (m, 8H), 2.85 (s, 3H), 1.89 (p, J = 6.0 Hz, 2H), 1.79 (p, J = 5.9 Hz, 2H).

5. DBU·*p*-HP

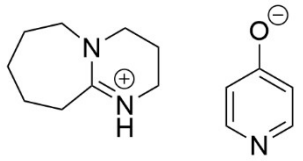

Yellow oil. **^{1}H NMR** (400 MHz, DMSO-d_6) δ 8.24 (s, 2H), 7.86 – 7.73 (m, 2H), 6.27 – 6.13 (m, 2H), 3.37 – 3.27 (m, 4H), 3.15 (d, J = 5.8 Hz, 4H), 1.79 (p, J = 5.8 Hz, 2H), 1.62 – 1.51 (m, 6H).

6. DMAP·*p*-HP

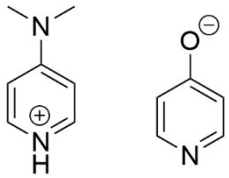

Yellow crystalline. **^{1}H NMR** (400 MHz, DMSO-d_6) δ 8.16 – 8.03 (m, 2H), 7.70 (d, J = 6.9 Hz, 2H), 6.66 – 6.53 (m, 2H), 6.17 (d, J = 6.8 Hz, 2H), 3.51 – 3.25 (m, 1H), 2.94 (s, 6H).

7. TMG·*p*-HP

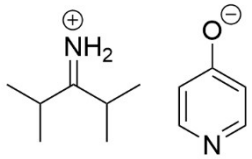

Yellow crystalline. **^{1}H NMR** (400 MHz, DMSO-d_6) δ 8.00 – 7.94 (m, 2H), 7.45 (s, 2H), 6.46 – 6.40 (m, 2H), 2.90 (s, 12H).

8. n-Bu$_4$N·*p*-HP

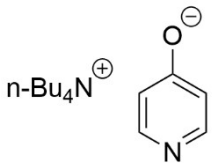

White oil. **^{1}H NMR** (400 MHz, DMSO-d_6) δ 7.68 – 7.51 (m, 2H), 6.01 – 5.89 (m, 2H),

3.31 – 3.04 (m, 8H), 1.55 (dq, J = 11.6, 7.2, 5.8 Hz, 8H), 1.30 (h, J = 7.4 Hz, 8H), 0.93 (t, J = 7.3 Hz, 12H).

9. TBD·BF_4

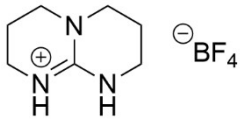

Yellow oil. **^{1}H NMR** (400 MHz, DMSO-d_6) δ 7.37 (s, 2H), 3.21 (dt, J = 36.7, 5.9 Hz, 8H), 1.86 (p, J = 5.9 Hz, 4H).

10. Me-TBD·*p*-HP

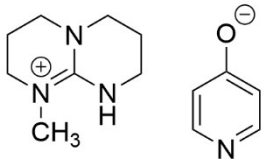

Yellow solid. **^{1}H NMR** (400 MHz, DMSO-d_6) δ 7.80 – 7.68 (m, 2H), 6.21 – 6.12 (m, 2H), 4.90 (s, 4H), 3.35 – 3.10 (m, 8H), 1.95 – 1.74 (m, 4H).

11. Me-TBD·BF_4

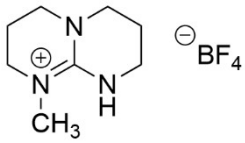

Yellow oil. **^{1}H NMR** (400 MHz, DMSO-d_6) δ 7.50 (d, J = 80.9 Hz, 1H), 3.41 – 3.18 (m, 8H), 2.92 (s, 3H), 1.90 (dp, J = 23.3, 6.0 Hz, 4H).

3. Characterization of catalysts (Figure S1–Figure S12)

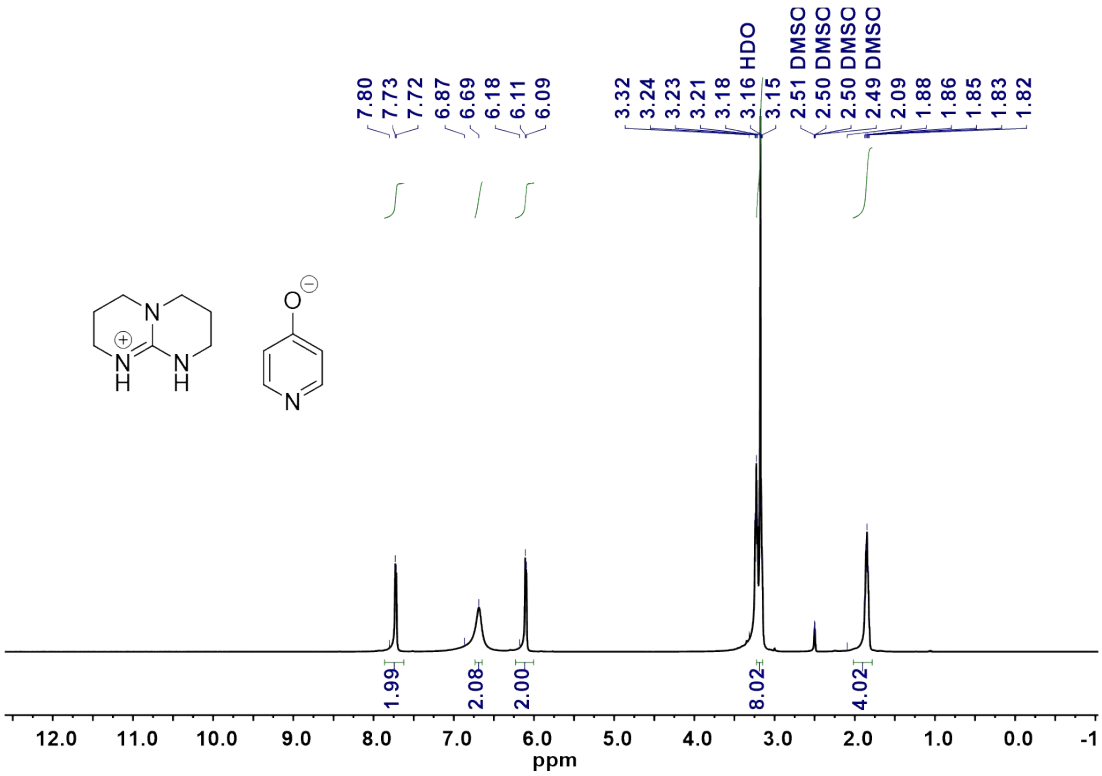

Figure S1. ^{1}H NMR spectrum (DMSO-d_6, 400 MHz) of **TBD·*p*-HP**

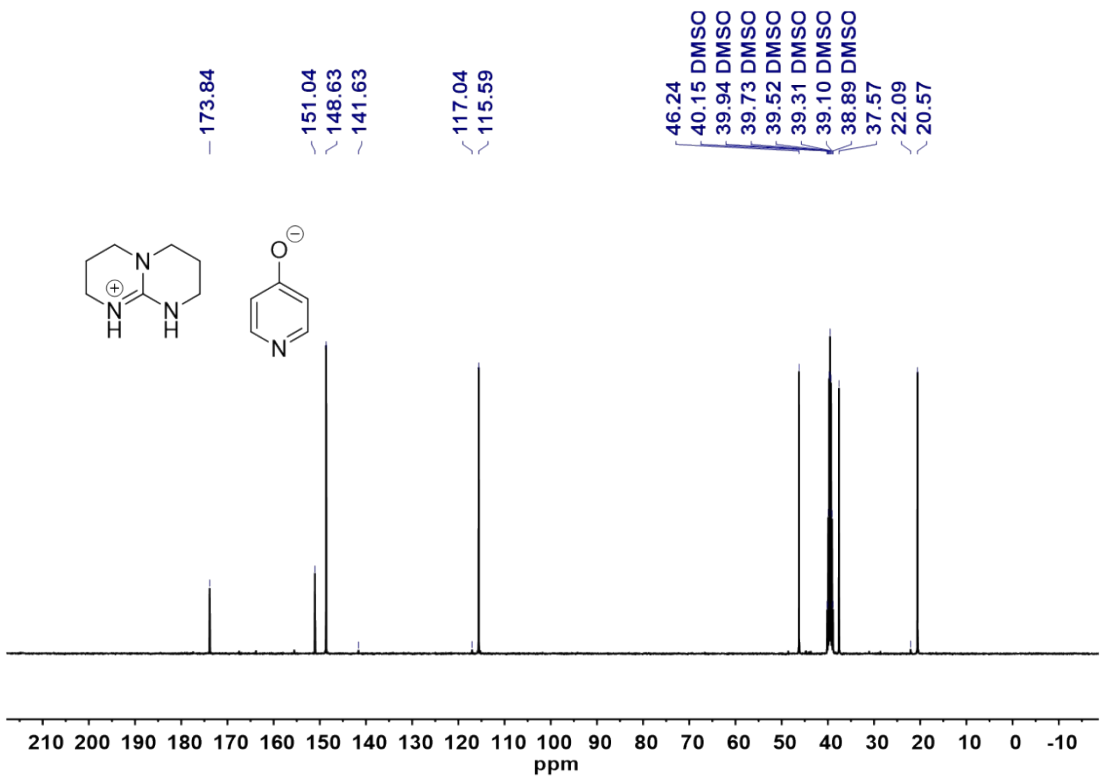

Figure S2. ^{13}C NMR spectrum (DMSO-d_6, 400 MHz) of **TBD·*p*-HP**

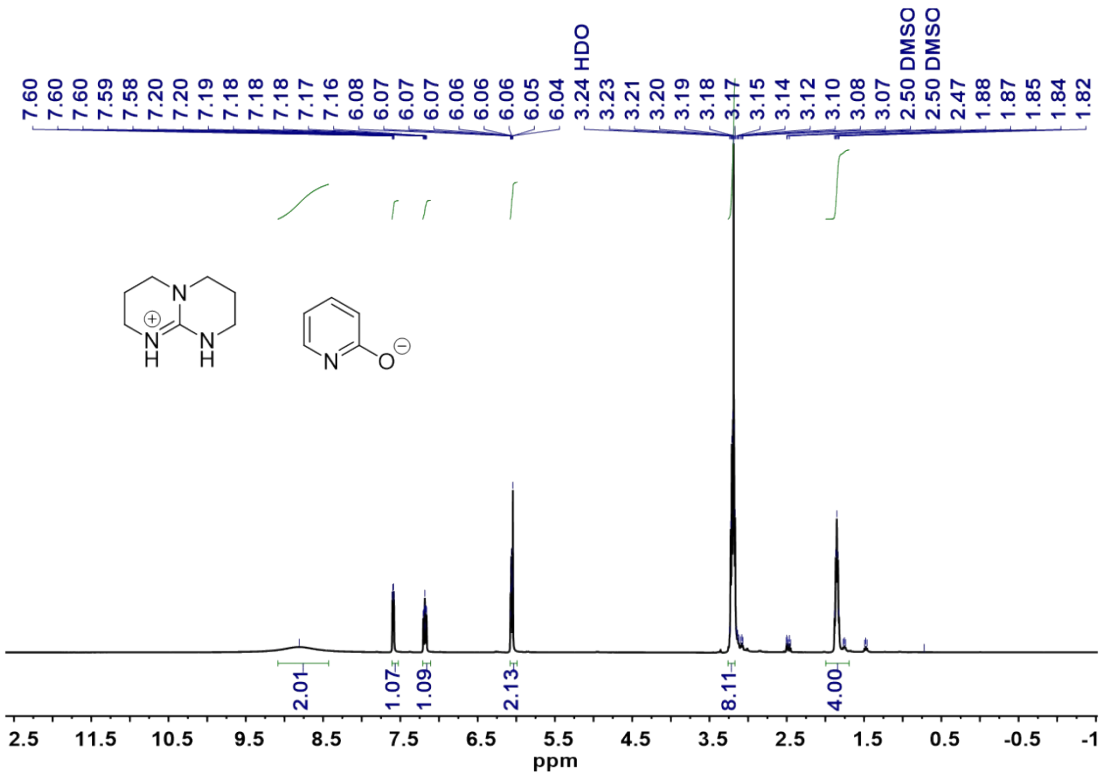

Figure S3. ^{1}H NMR spectrum (DMSO-d_6, 400 MHz) of **TBD·*o*-HP**

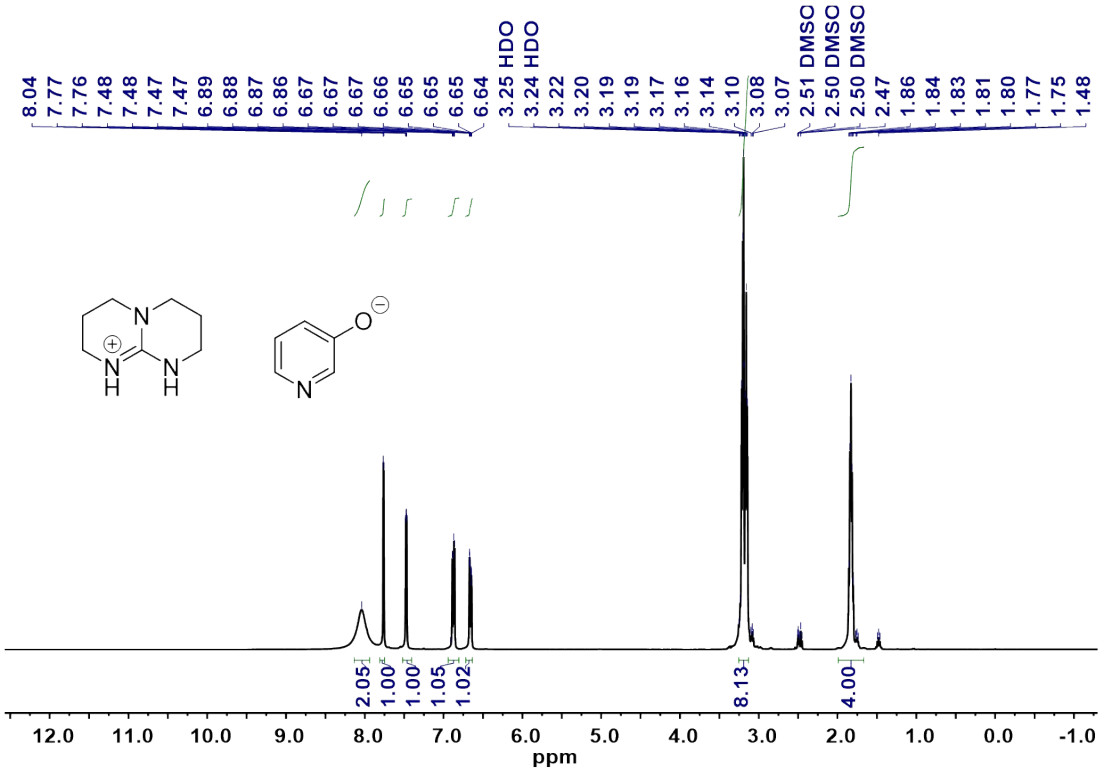

Figure S4. ^{1}H NMR spectrum (DMSO-d_6, 400 MHz) of **TBD·*m*-HP**

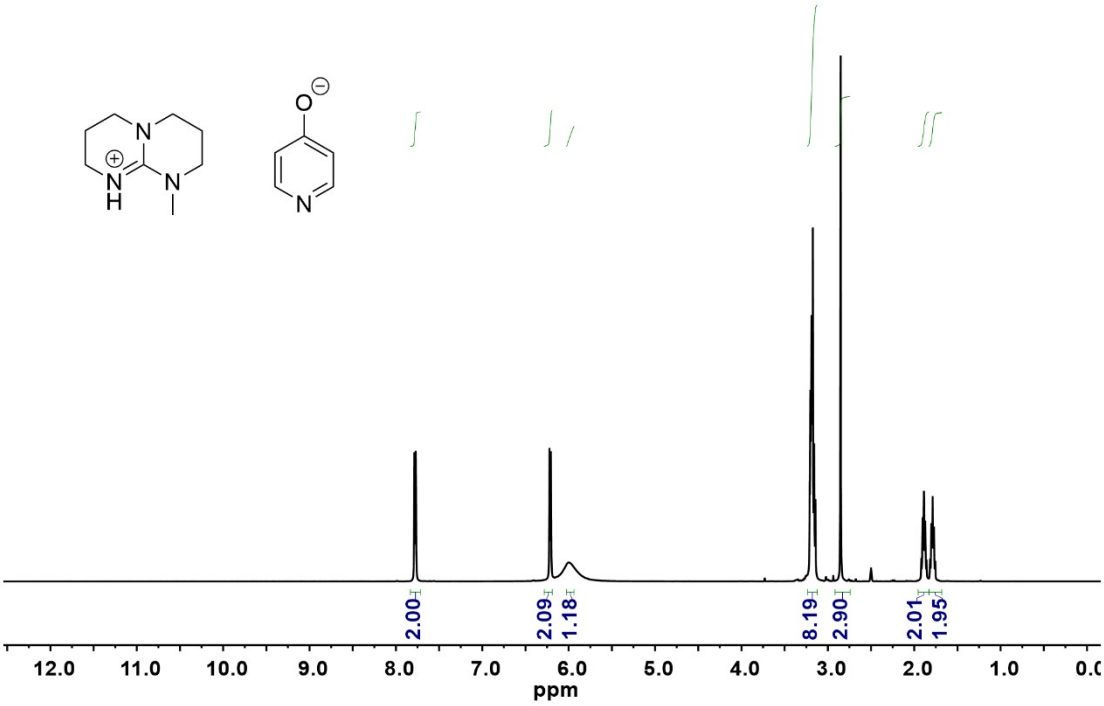

Figure S5. ^{1}H NMR spectrum (DMSO-d_6, 400 MHz) of **MTBD·*p*-HP**

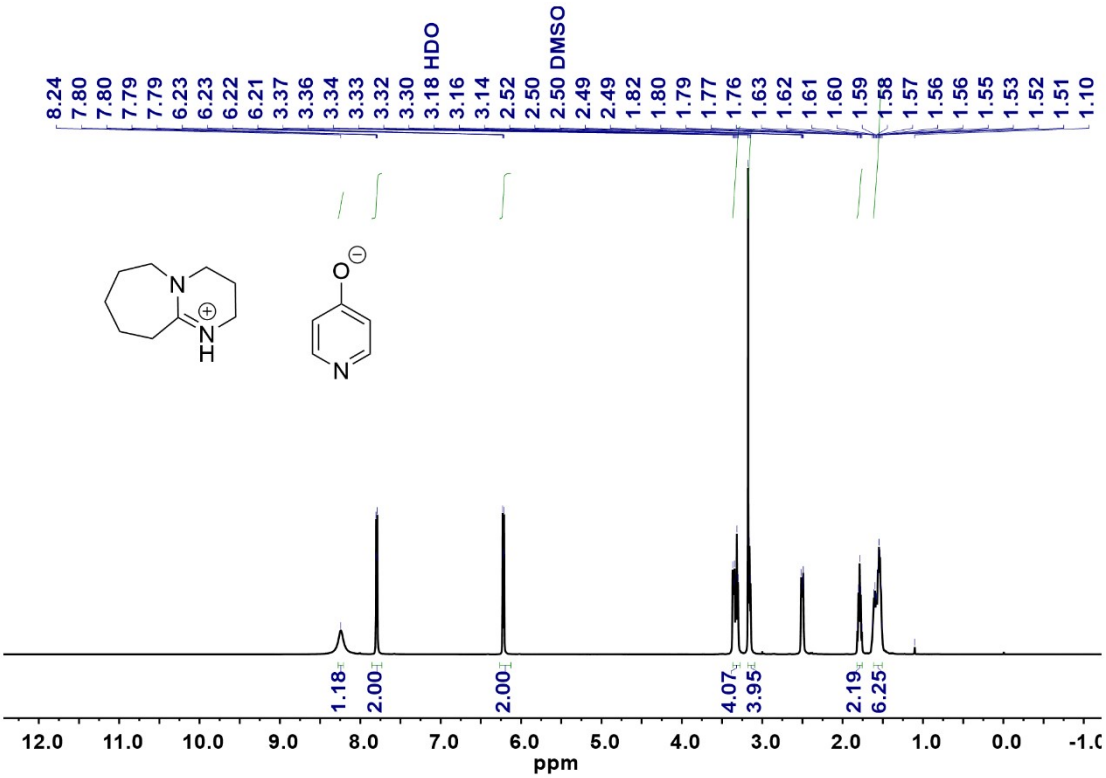

Figure S6. ^{1}H NMR spectrum (DMSO-d_6, 400 MHz) of **DBU·*p*-HP**

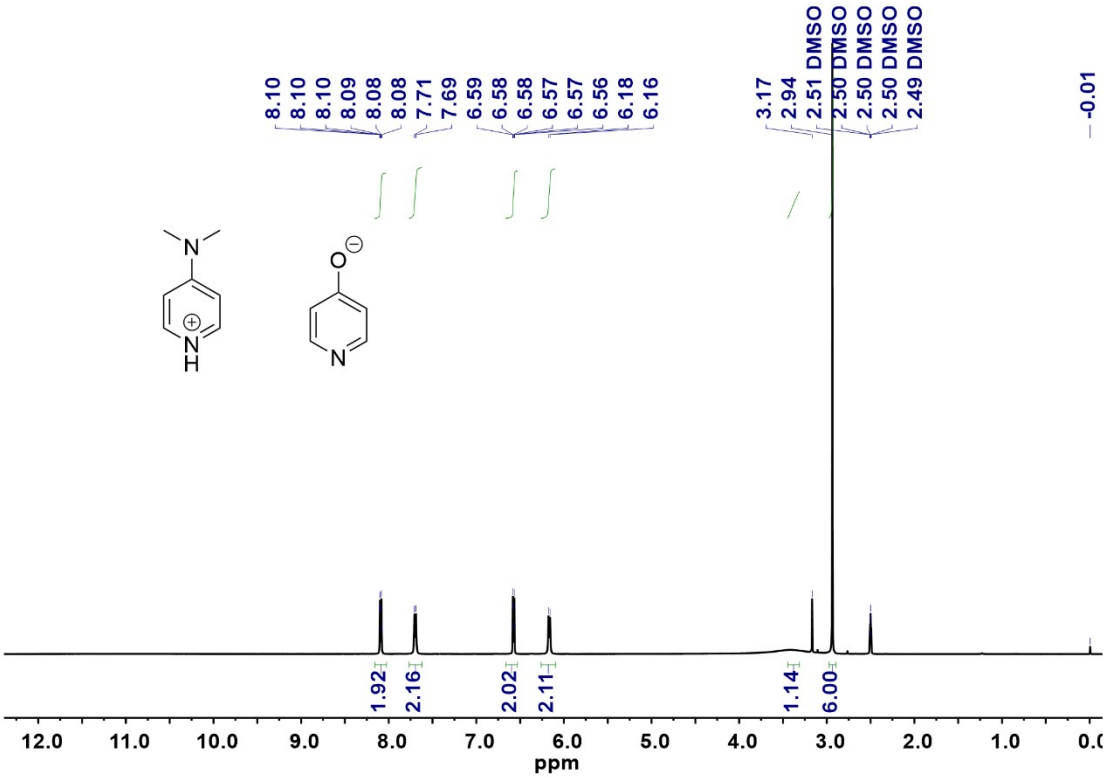

Figure S7. ^{1}H NMR spectrum (DMSO-d_6, 400 MHz) of **DMAP·*p*-HP**

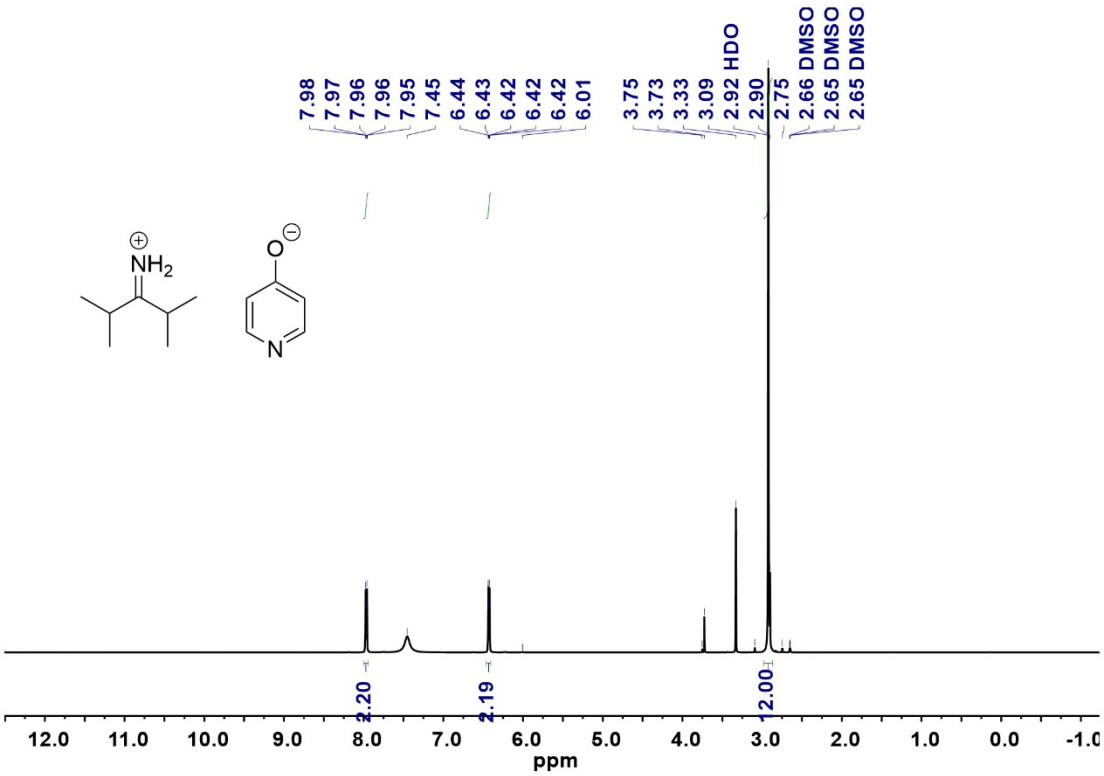

Figure S8. ^{1}H NMR spectrum (DMSO-d_6, 400 MHz) of **TMG·*p*-HP**

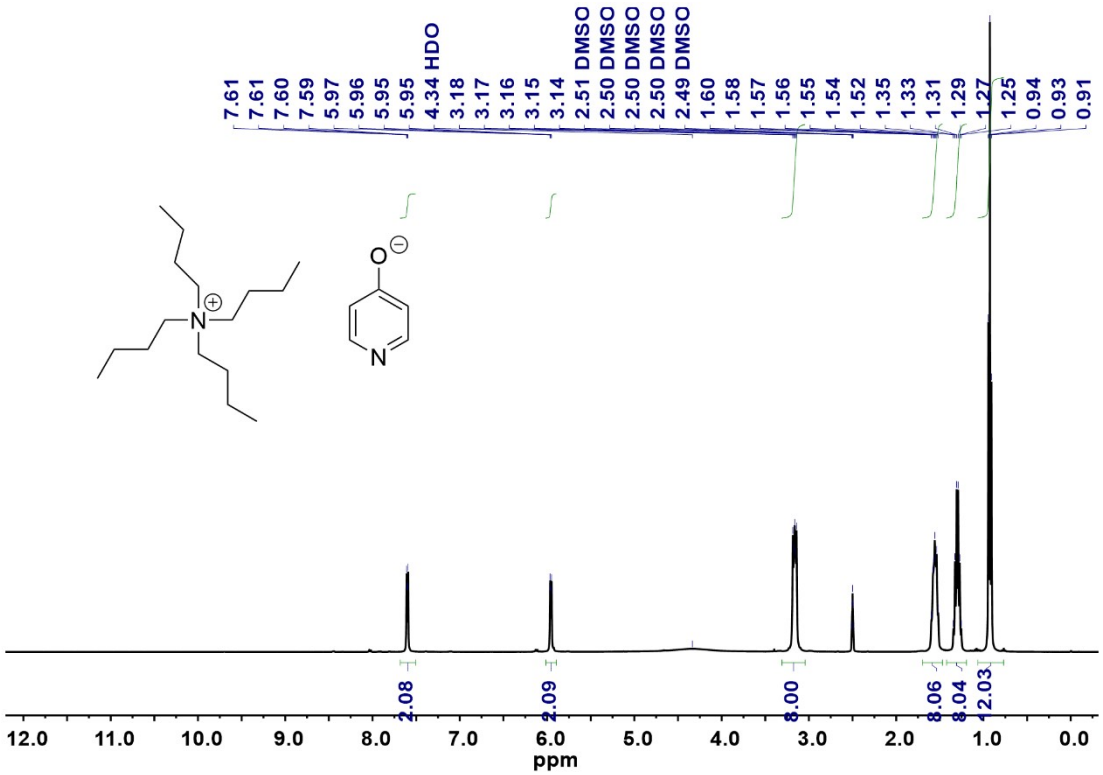

Figure S9. ^{1}H NMR spectrum (DMSO-d_6, 400 MHz) of **n-BU$_4$N·*p*-HP**

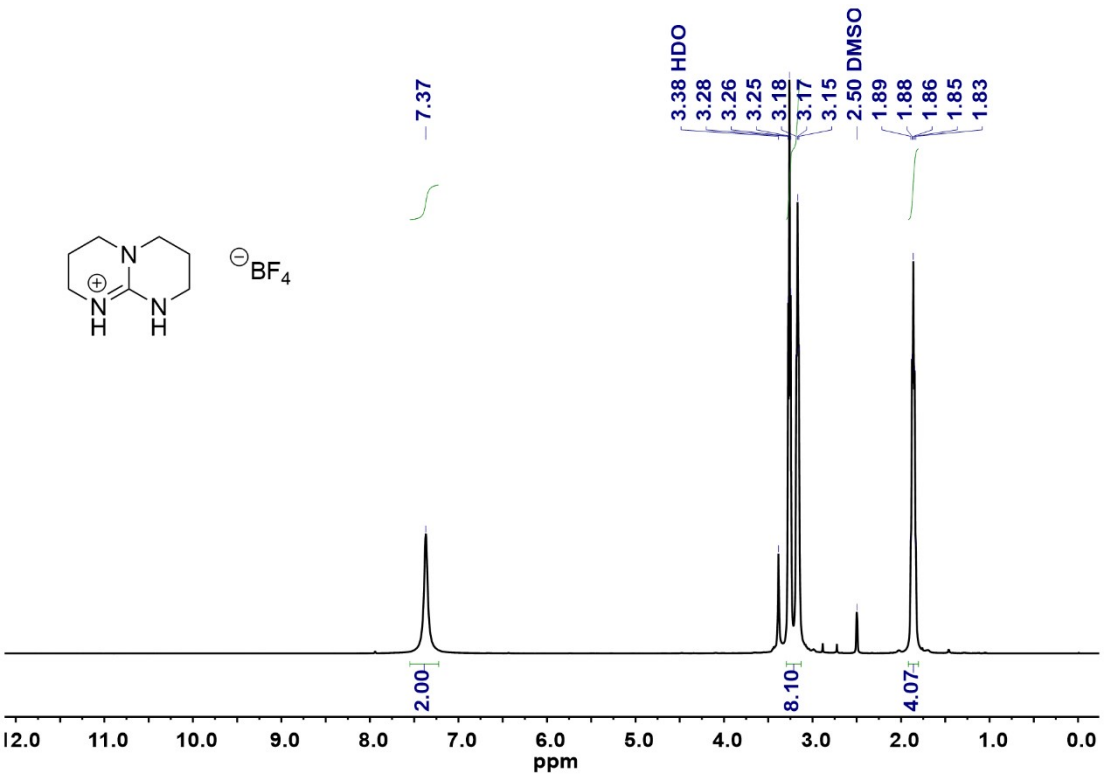

Figure S10. ^{1}H NMR spectrum (DMSO-d_6, 400 MHz) of **TBD·BF$_4$**

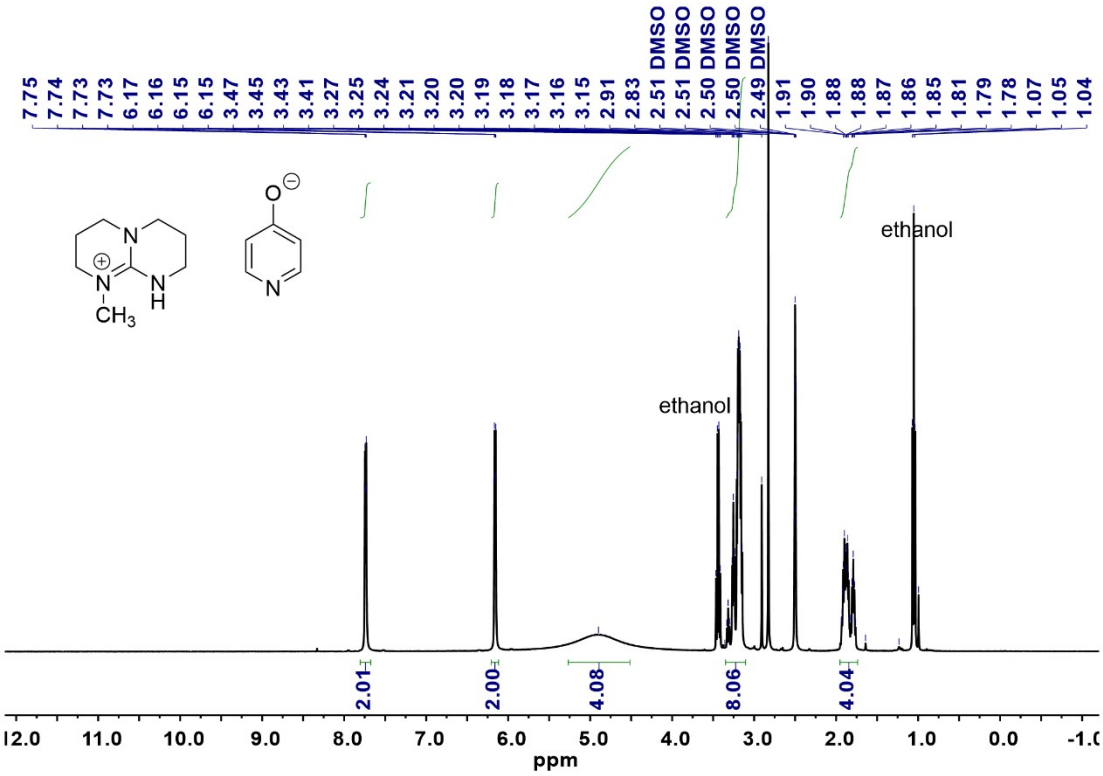

Figure S11. ^{1}H NMR spectrum (DMSO-d_6, 400 MHz) of **Me-TBD·*p*-HP**

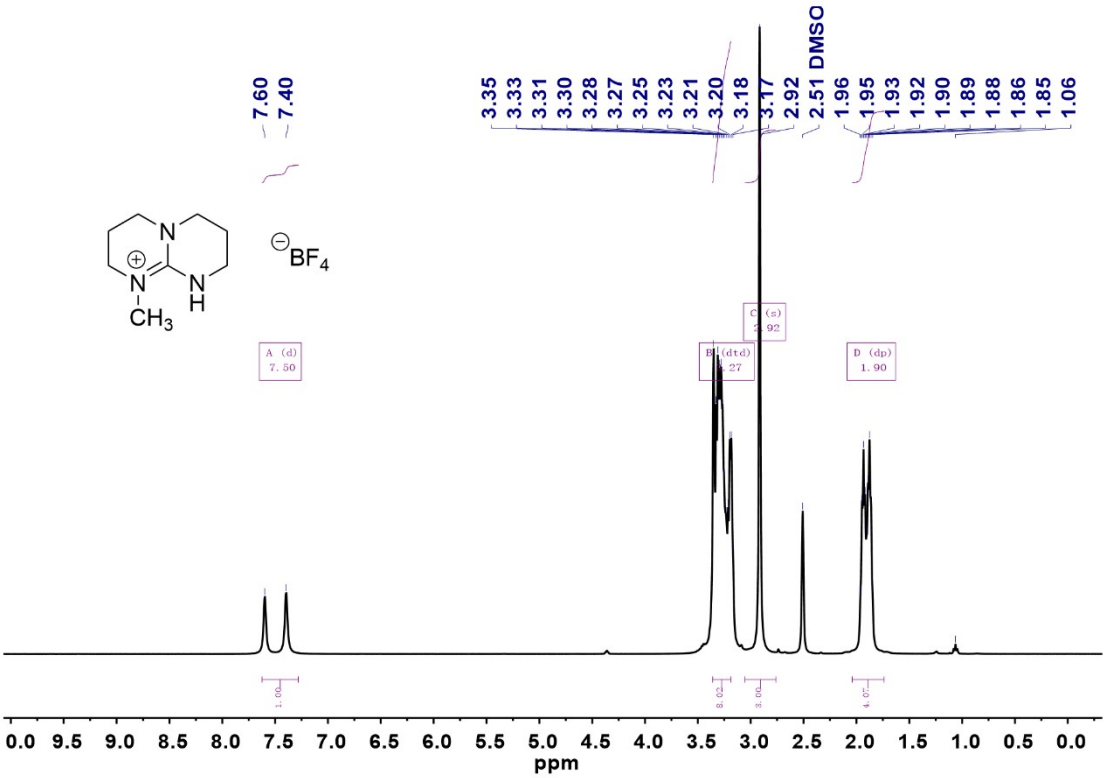

Figure S12. ^{1}H NMR spectrum (DMSO-d_6, 400 MHz) of **Me-TBD·BF$_4$**

4. Spectral data for the cyclic carbonates

4-(Chloromethyl)-1,3-dioxolan-2-one [1]

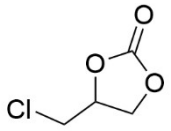

^{1}H NMR (400 MHz, $CDCl_3$) δ 4.97 (dtd, *J* = 8.1, 5.6, 3.7 Hz, 1H), 4.59 (t, *J* = 8.6 Hz, 1H), 4.40 (dd, *J* = 8.9, 5.8 Hz, 1H), 3.83–3.68 (m, 2H). **^{13}C NMR** (101 MHz, $CDCl_3$) δ 154.33, 74.38, 67.07, 43.80.

4-(Bromomethyl)-1,3-dioxolan-2-one [1]

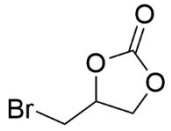

^{1}H NMR (400 MHz, $CDCl_3$) δ 4.95 (dtd, *J* = 8.1, 5.9, 4.7 Hz, 1H), 4.60 (dd, *J* = 8.9, 8.1 Hz, 1H), 4.36 (dd, *J* = 8.9, 5.9 Hz, 1H), 3.63–3.52 (m, 2H). **^{13}C NMR** (101 MHz, $CDCl_3$) δ 154.22, 74.07, 68.24, 31.32.

4-(Methoxymethyl)-1,3-dioxolan-2-one [1]

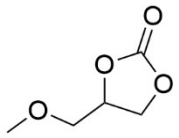

^{1}H NMR (400 MHz, $CDCl_3$) δ 4.85–4.75 (m, 1H), 4.49 (t, *J* = 8.4 Hz, 1H), 4.37 (dd, *J* = 8.4, 6.1 Hz, 1H), 3.63 (dd, *J* = 11.0, 3.8 Hz, 1H), 3.55 (dd, *J* = 11.0, 3.8 Hz, 1H), 3.41 (s, 3H). **^{13}C NMR** (101 MHz, $CDCl_3$) δ 155.08, 75.10, 71.54, 66.26, 59.72.

4-((Allyloxy)methyl)-1,3-dioxolan-2-one [1]

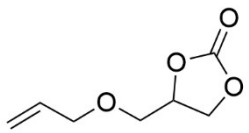

^{1}H NMR (400 MHz, $CDCl_3$) δ 5.86 (ddt, *J* = 17.3, 10.4, 5.6 Hz, 1H), 5.45–5.10 (m, 2H), 4.81 (ddt, *J* = 7.9, 6.0, 3.8 Hz, 1H), 4.49 (t, *J* = 8.4 Hz, 1H), 4.39 (dd, *J* = 8.4, 6.0 Hz, 1H), 4.11–3.98 (m, 2H), 3.76–3.41 (m, 2H). **^{13}C NMR** (101 MHz, $CDCl_3$) δ 155.07, 133.76, 118.03, 75.14, 72.68, 68.92, 66.37.

4-(*tert*-Butoxymethyl)-1,3-dioxolan-2-one [1]

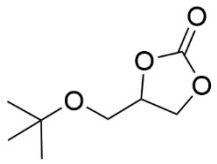

^{1}H NMR (400 MHz, $CDCl_3$) δ 4.76 (dddd, *J* = 8.1, 5.8, 4.5, 3.6 Hz, 1H), 4.46 (t, *J* = 8.2 Hz, 1H), 4.42–4.33 (m, 1H), 3.61 (dd, *J* = 10.3, 4.6 Hz, 1H), 3.52 (ddt, *J* = 10.4, 3.6, 1.0 Hz, 1H), 1.19 (s, 9H). **^{13}C NMR** (101 MHz, $CDCl_3$) δ 155.30, 75.28, 74.01, 66.69, 61.39, 27.40.

4-(Phenoxymethyl)-1,3-dioxolan-2-one [1]

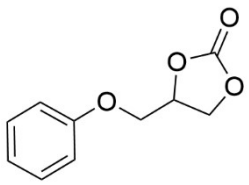

^{1}H NMR (400 MHz, $CDCl_3$) δ 7.31 (ddt, *J* = 9.6, 7.2, 2.1 Hz, 2H), 7.02 (td, *J* = 7.4, 1.0 Hz, 1H), 6.94–6.88 (m, 2H), 5.03 (ddt, *J* = 8.1, 5.9, 3.9 Hz, 1H), 4.65–4.51 (m, 2H), 4.24 (dd, *J* = 10.6, 4.1 Hz, 1H), 4.14 (dd, *J* = 10.6, 3.6 Hz, 1H). **^{13}C NMR** (101 MHz, $CDCl_3$) δ 157.87,

154.83, 129.82, 122.11, 114.72, 74.25, 66.97, 66.35.

4-Butyl-1,3-dioxolan-2-one [2]

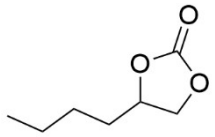

^{1}H NMR (400 MHz, $CDCl_3$) δ 4.70 (qd, *J* = 7.5, 5.4 Hz, 1H), 4.52 (t, *J* = 8.1 Hz, 1H), 4.06 (dd, *J* = 8.4, 7.2 Hz, 1H), 1.86–1.74 (m, 1H), 1.73–1.61 (m, 1H), 1.50–1.24 (m, 4H), 0.91 (t, *J* = 6.9 Hz, 3H). **^{13}C NMR** (101 MHz, $CDCl_3$) δ 155.23, 77.17, 69.51, 33.66, 26.53, 22.35, 13.90.

4-(But-3-en-1-yl)-1,3-dioxolan-2-one [3]

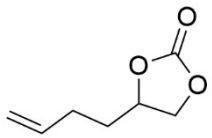

^{1}H NMR (400 MHz, $CDCl_3$) δ 5.76 (ddt, *J* = 16.9, 10.2, 6.6 Hz, 1H), 5.11–4.98 (m, 2H), 4.71 (qd, *J* = 7.7, 5.1 Hz, 1H), 4.51 (t, *J* = 8.2 Hz, 1H), 4.06 (dd, *J* = 8.5, 7.2 Hz, 1H), 2.30–2.08 (m, 2H), 1.90 (dtd, *J* = 14.0, 8.1, 5.9 Hz, 1H), 1.75 (dddd, *J* = 14.0, 8.8, 7.0, 5.1 Hz, 1H). **^{13}C NMR** (101 MHz, $CDCl_3$) δ 155.06, 136.18, 116.47, 76.43, 69.41, 33.11, 28.72.

4-Phenyl-1,3-dioxolan-2-one [1]

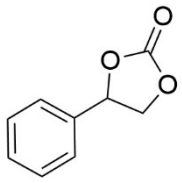

^{1}H NMR (400 MHz, $CDCl_3$) δ 7.43 (qd, *J* = 3.9, 2.0 Hz, 3H), 7.39–7.32 (m, 2H), 5.68 (t, *J* = 8.0 Hz, 1H), 4.80 (t, *J* = 8.4 Hz, 1H), 4.34 (dd, *J* = 8.6, 7.8 Hz, 1H). **^{13}C NMR** (101 MHz,

$CDCl_3$) δ 154.96, 135.89, 129.83, 129.33, 125.99, 78.10, 71.28.

4-((*o*-Tolyloxy)methyl)-1,3-dioxolan-2-one [1]

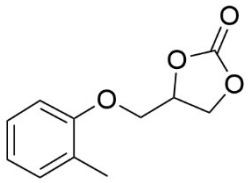

^{1}H NMR (400 MHz, $CDCl_3$) δ 7.16 (ddt, *J* = 7.4, 4.0, 2.6 Hz, 2H), 6.93 (td, *J* = 7.4, 1.1 Hz, 1H), 6.81–6.75 (m, 1H), 5.10–5.00 (m, 1H), 4.67–4.54 (m, 2H), 4.26 (dd, *J* = 10.6, 3.5 Hz, 1H), 4.13 (dd, *J* = 10.6, 3.0 Hz, 1H), 2.22 (s, 3H). **^{13}C NMR** (101 MHz, $CDCl_3$) δ 155.85, 154.96, 131.19, 127.18, 127.00, 121.75, 110.89, 74.34, 67.08, 66.35, 16.08.

4,4'-(((propane-2,2-diylbis(4,1-phenylene))bis(methylene))bis(oxy))bis(1,3-dioxolan-2-one) [2]

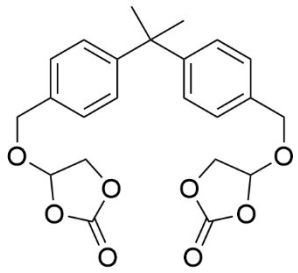

^{1}H NMR (400 MHz, $CDCl_3$) δ 7.19 – 7.08 (m, 4H), 6.85 – 6.75 (m, 4H), 5.01 (ddt, J = 8.1, 5.9, 4.0 Hz, 2H), 4.60 (t, J = 8.4 Hz, 2H), 4.52 (dd, J = 8.5, 5.9 Hz, 2H), 4.21 (dd, J = 10.6, 4.3 Hz, 2H), 4.12 (dd, J = 10.6, 3.6 Hz, 2H), 1.63 (s, 6H). **^{13}C NMR** (101 MHz, $CDCl_3$) δ 155.66, 154.62, 144.36, 127.94, 114.07, 74.10, 66.94, 66.24, 41.85, 30.97.

5. Characterization of cyclic carbonates (Figure S13 – Figure S34)

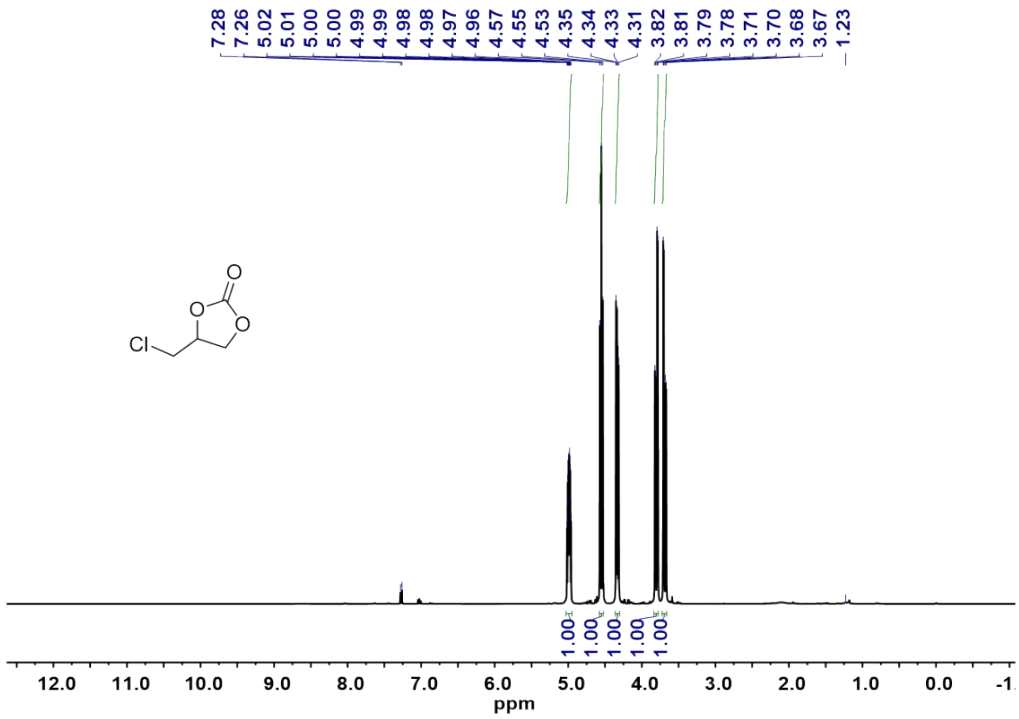

Figure S13. ^{1}H NMR spectrum ($CDCl_3$, 400 MHz) of 3-Chloropropylene carbonate (obtained from crude reaction mass)

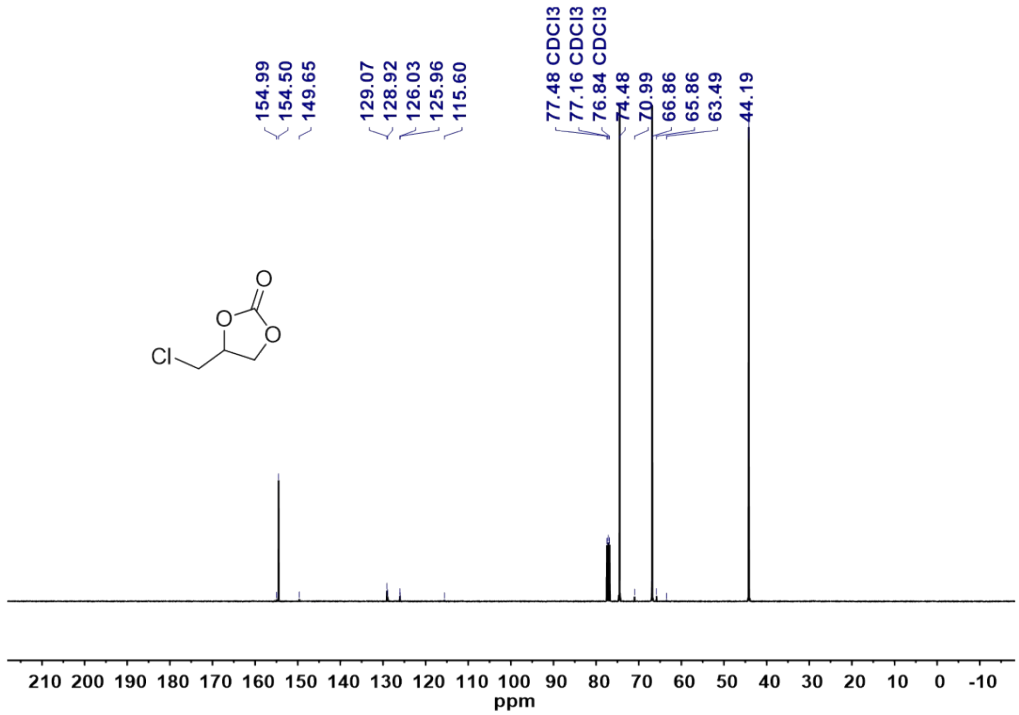

Figure S14. ^{13}C NMR spectrum ($CDCl_3$, 400 MHz) of 3-Chloropropylene carbonate (obtained from crude reaction mass)

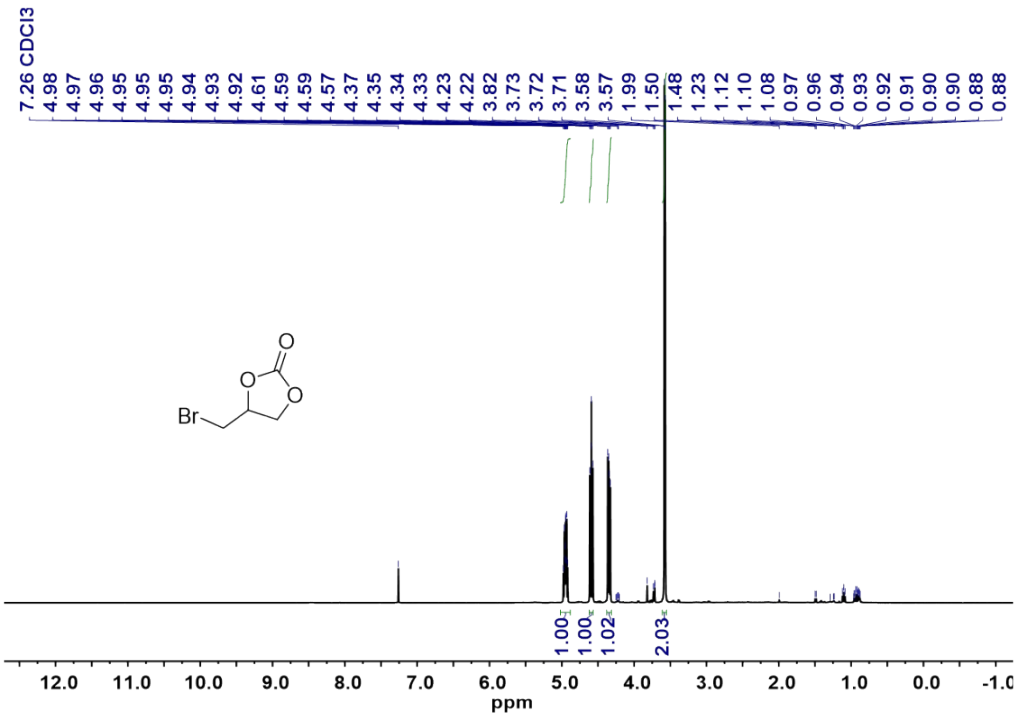

Figure S15. ^{1}H NMR spectrum ($CDCl_3$, 400 MHz) of 4-(bromomethyl)-1,3-dioxolan-2-one (obtained from crude reaction mass)

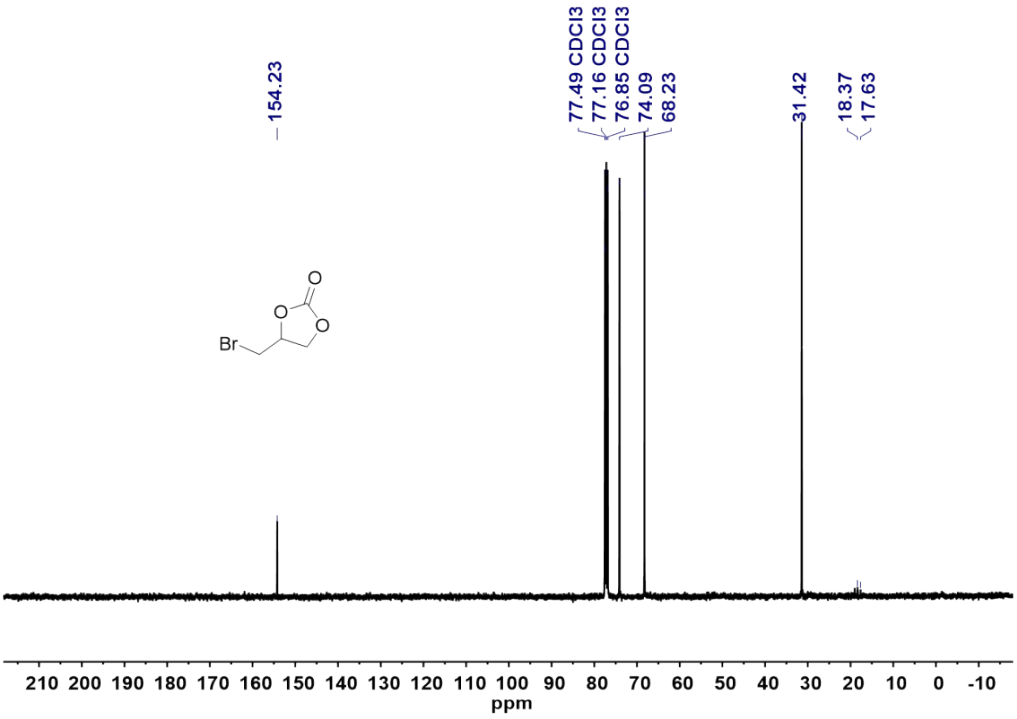

Figure S16. ^{13}C NMR spectrum ($CDCl_3$, 400 MHz) of 4-(bromomethyl)-1,3-dioxolan-2-one (obtained from crude reaction mass)

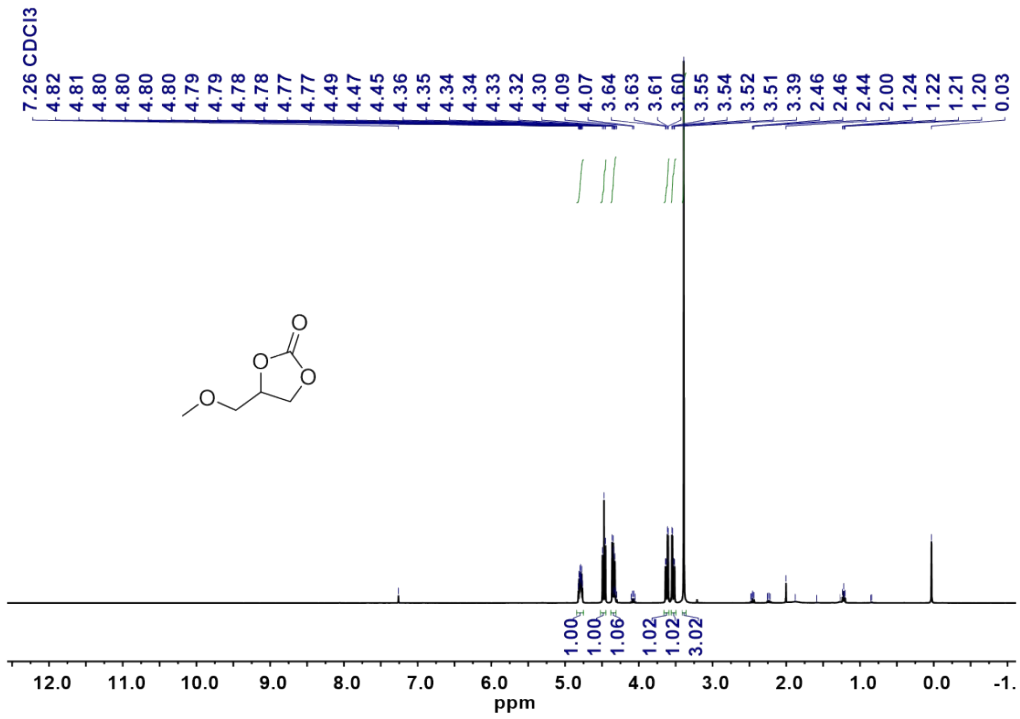

Figure S17. ^{1}H NMR spectrum ($CDCl_3$, 400 MHz) of 4-(methoxymethyl)-1,3-dioxolan-2-one (obtained from crude reaction mass)

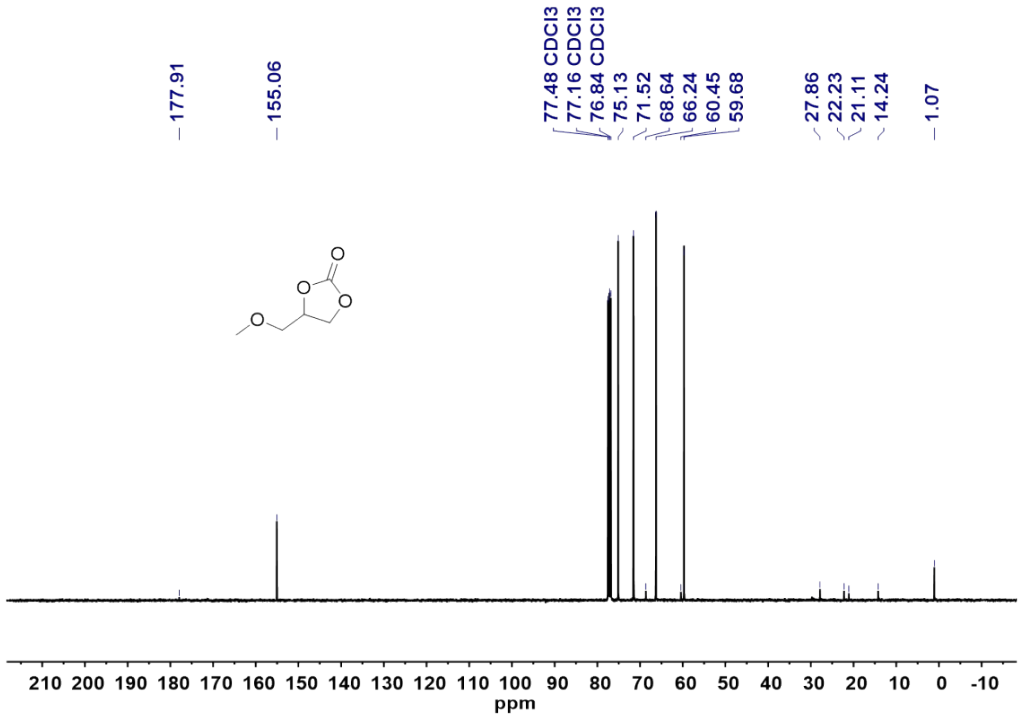

Figure S18. ^{13}C NMR spectrum ($CDCl_3$, 400 MHz) of 4-(methoxymethyl)-1,3-dioxolan-2-one (obtained from crude reaction mass)

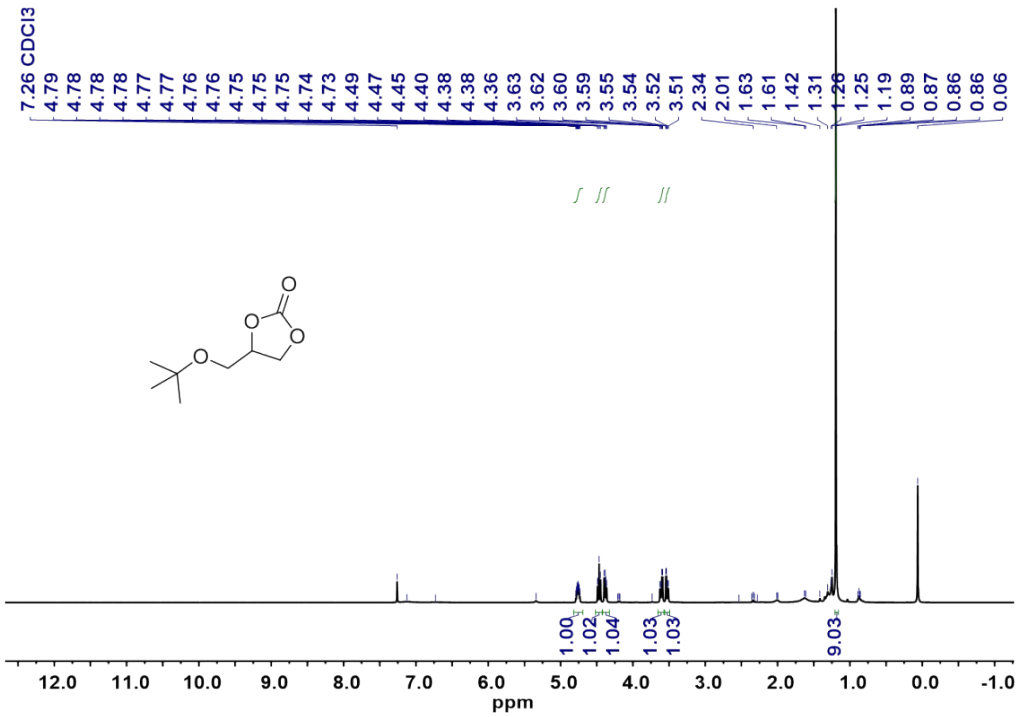

Figure S19 ^{1}H NMR spectrum ($CDCl_3$, 400 MHz) of 4-(tert-butoxymethyl)-1,3-dioxolan-2-one (obtained from crude reaction mass)

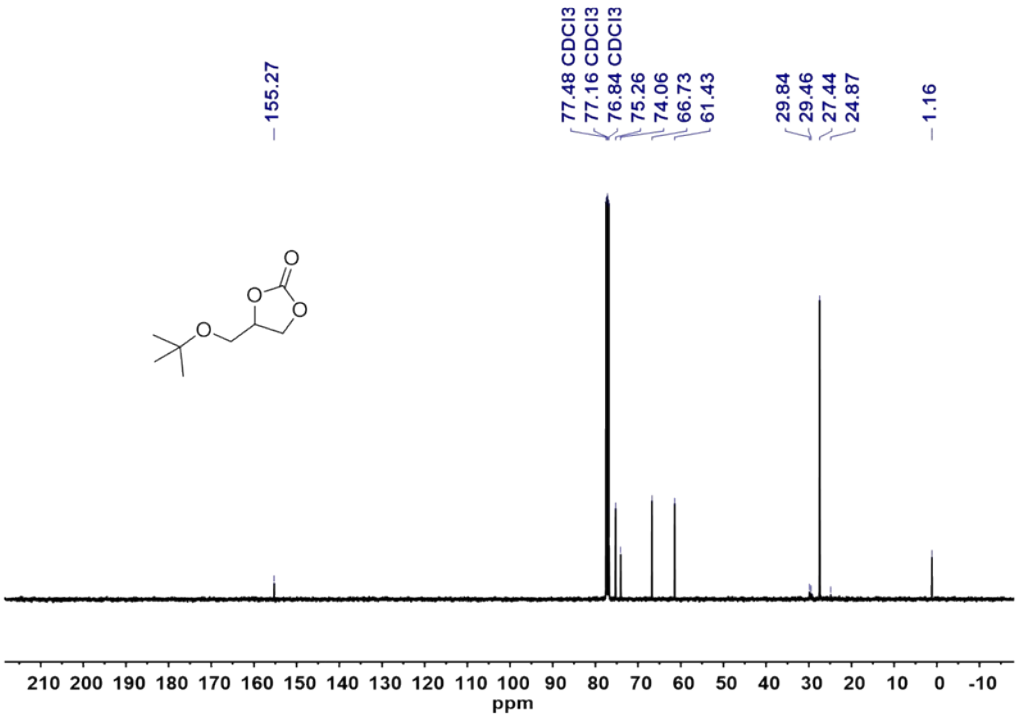

Figure S20. ^{13}C NMR spectrum ($CDCl_3$, 400 MHz) of 4-(tert-butoxymethyl)-1,3-dioxolan-2-one (obtained from crude reaction mass)

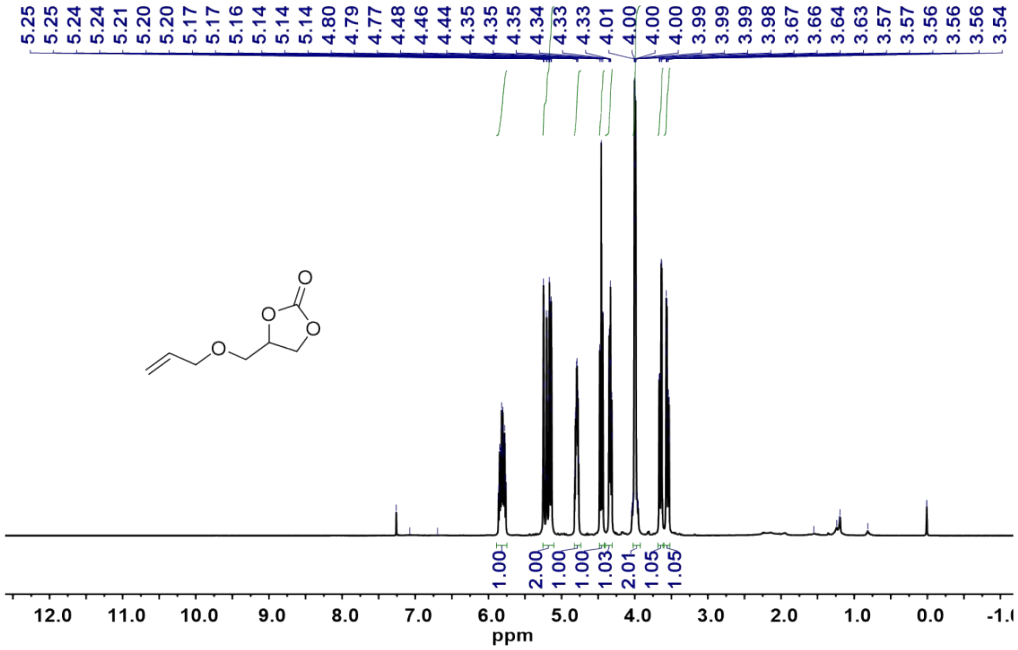

Figure S21. ^{1}H NMR spectrum ($CDCl_3$, 400 MHz) of 4-((allyloxy)methyl)-1,3-dioxolan-2-one (obtained from crude reaction mass)

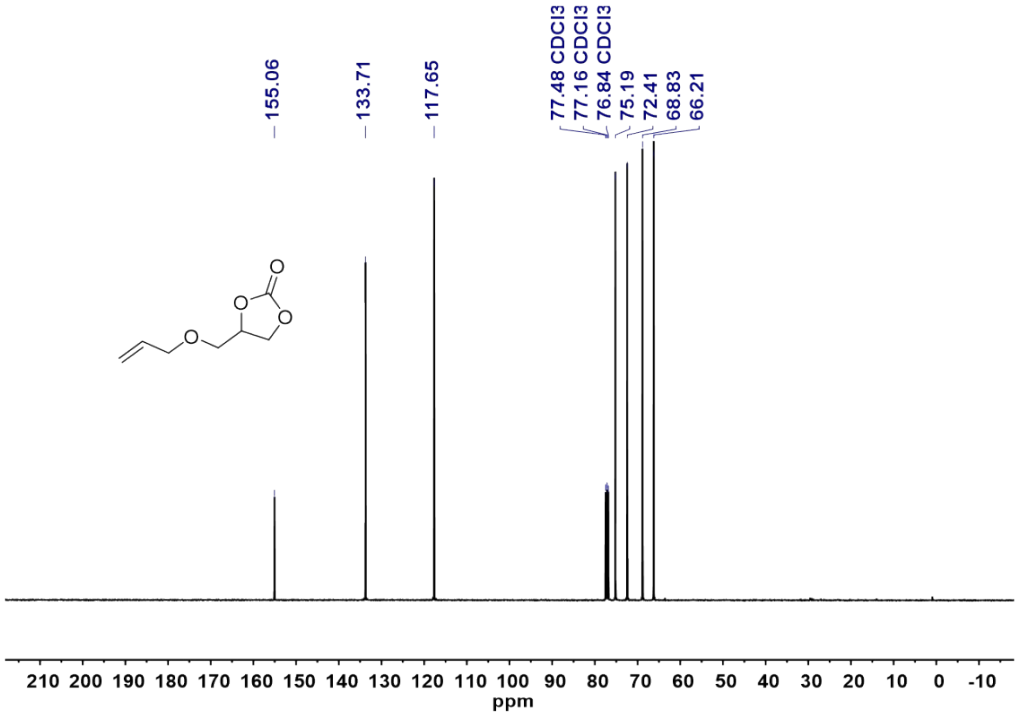

Figure S22. ^{13}C NMR spectrum ($CDCl_3$, 400 MHz) of 4-((allyloxy)methyl)-1,3-dioxolan-2-one (obtained from crude reaction mass)

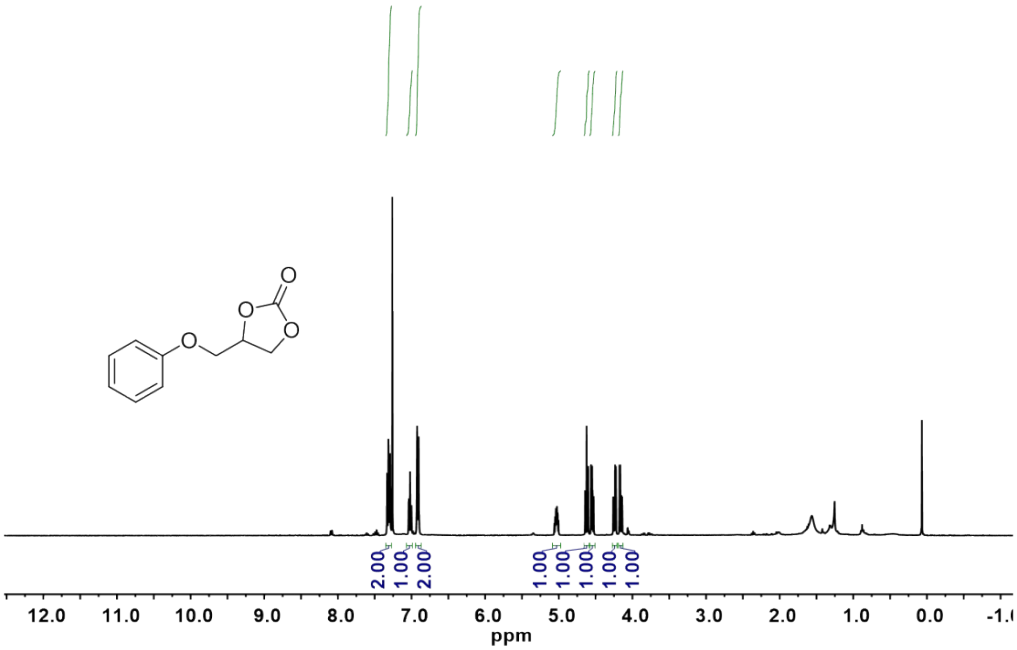

Figure S23 ^{1}H NMR spectrum ($CDCl_3$, 400 MHz) of 4-(phenoxymethyl)-1,3-dioxolan-2-one (obtained from crude reaction mass)

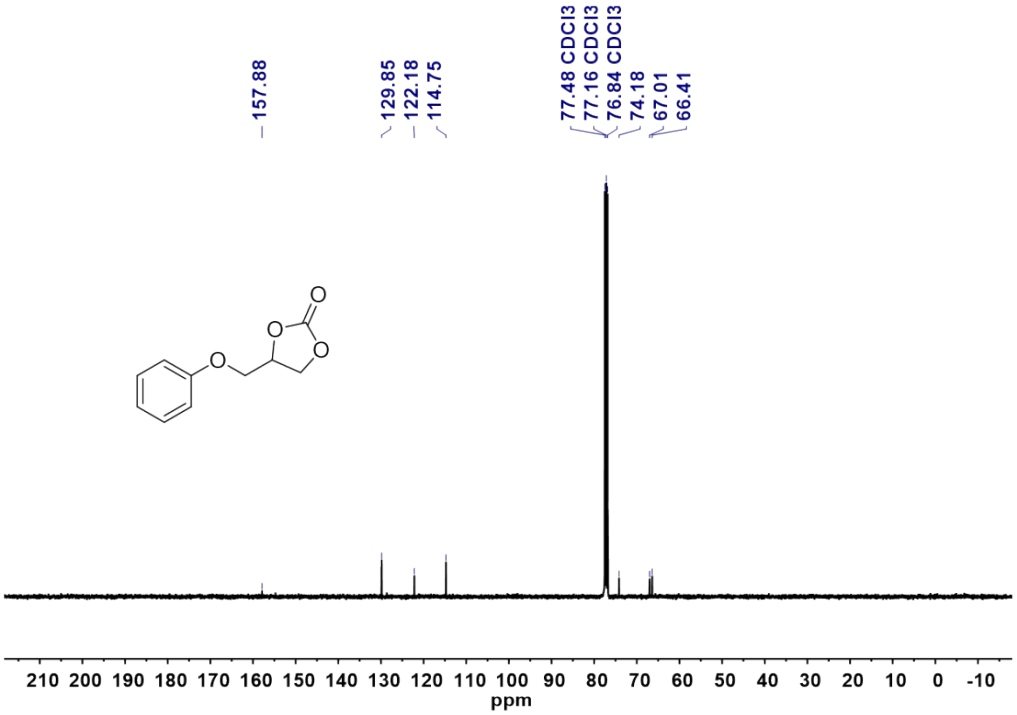

Figure S24. ^{13}C NMR spectrum ($CDCl_3$, 400 MHz) of 4-(phenoxymethyl)-1,3-dioxolan-2-one (obtained from crude reaction mass)

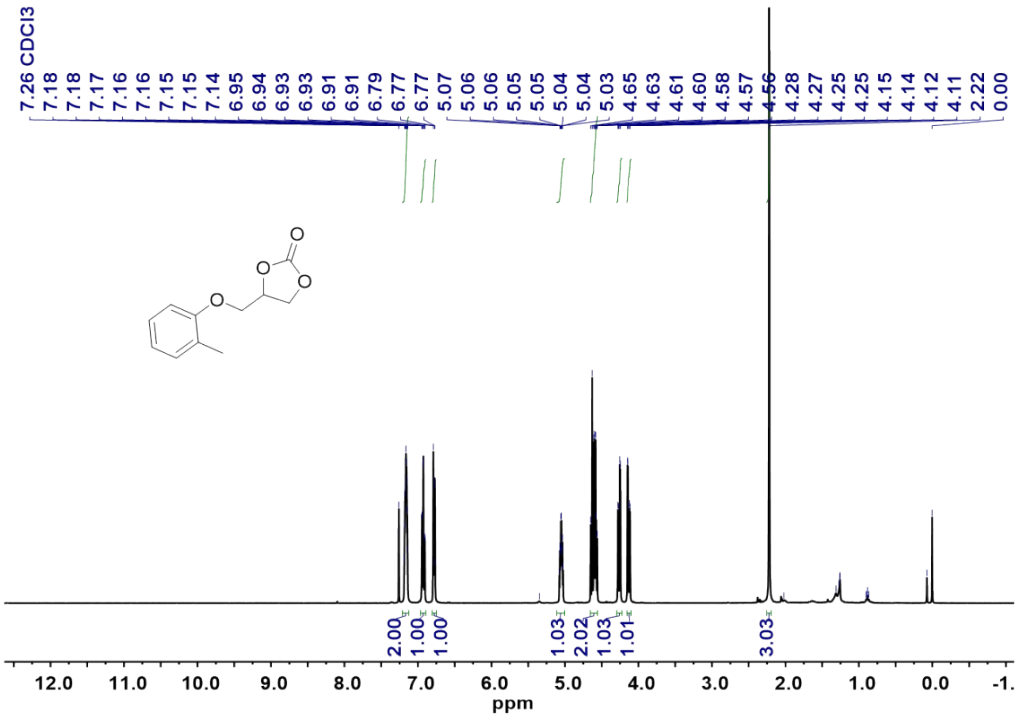

Figure S25 ^{1}H NMR spectrum ($CDCl_3$, 400 MHz) of 4-((o-tolyloxy) methyl)-1,3-dioxolan-2-one (obtained from crude reaction mass)

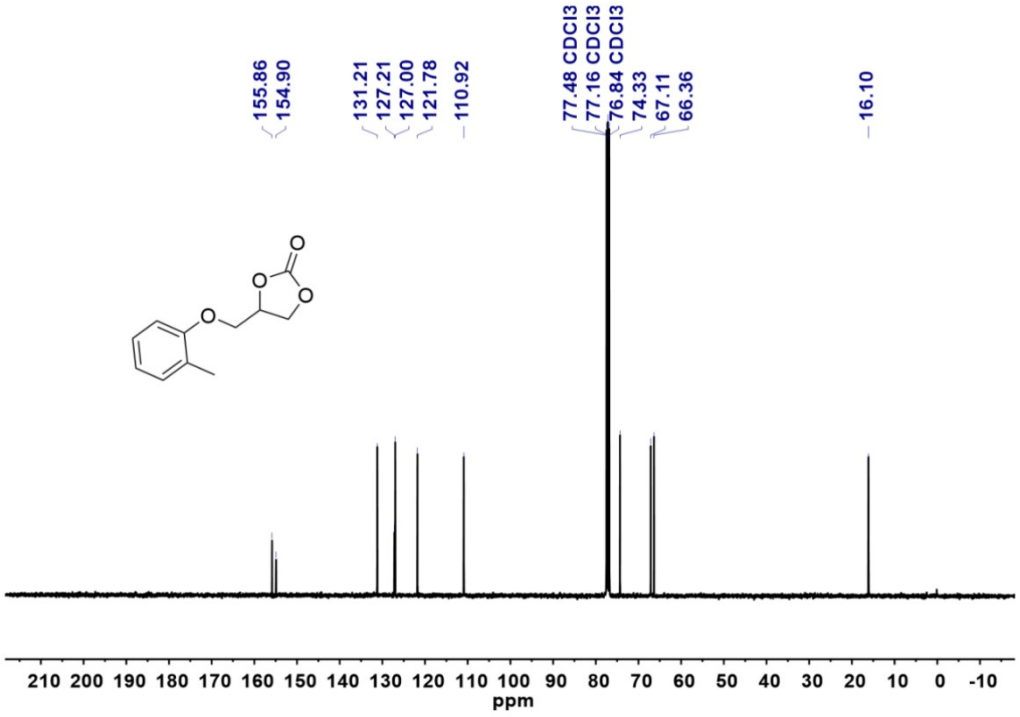

Figure S26 ^{13}C NMR spectrum ($CDCl_3$, 400 MHz) of 4-((o-tolyloxy) methyl)-1,3-dioxolan-2-one (obtained from crude reaction mass)

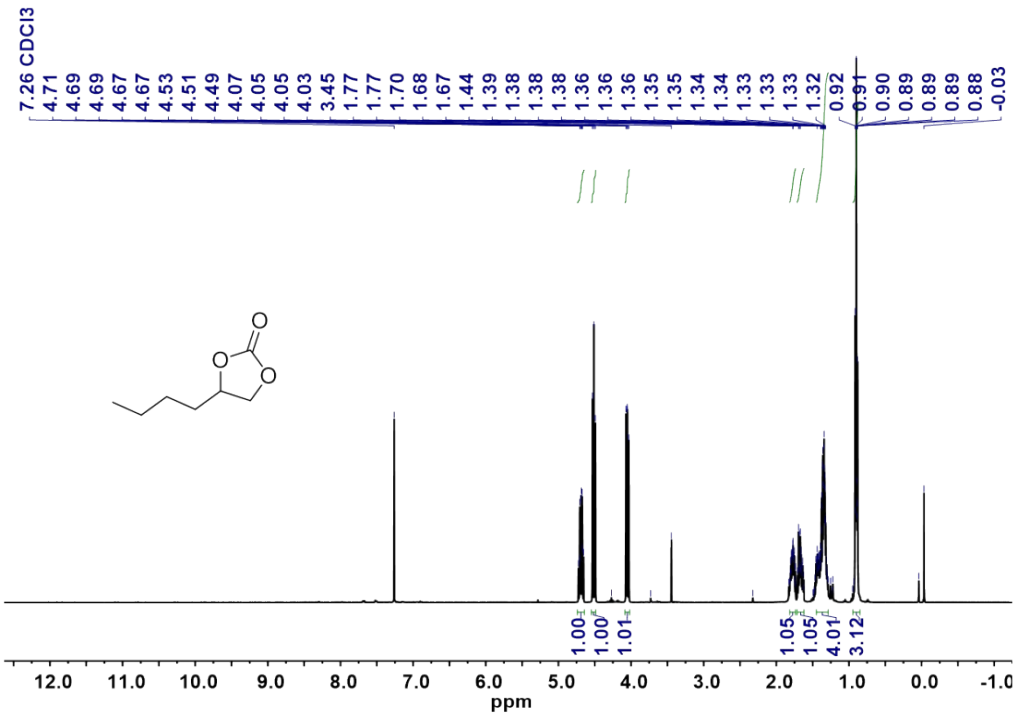

Figure S27. ^{1}H NMR spectrum ($CDCl_3$, 400 MHz) of 4-butyl-1,3-dioxane-2-one (obtained from crude reaction mass)

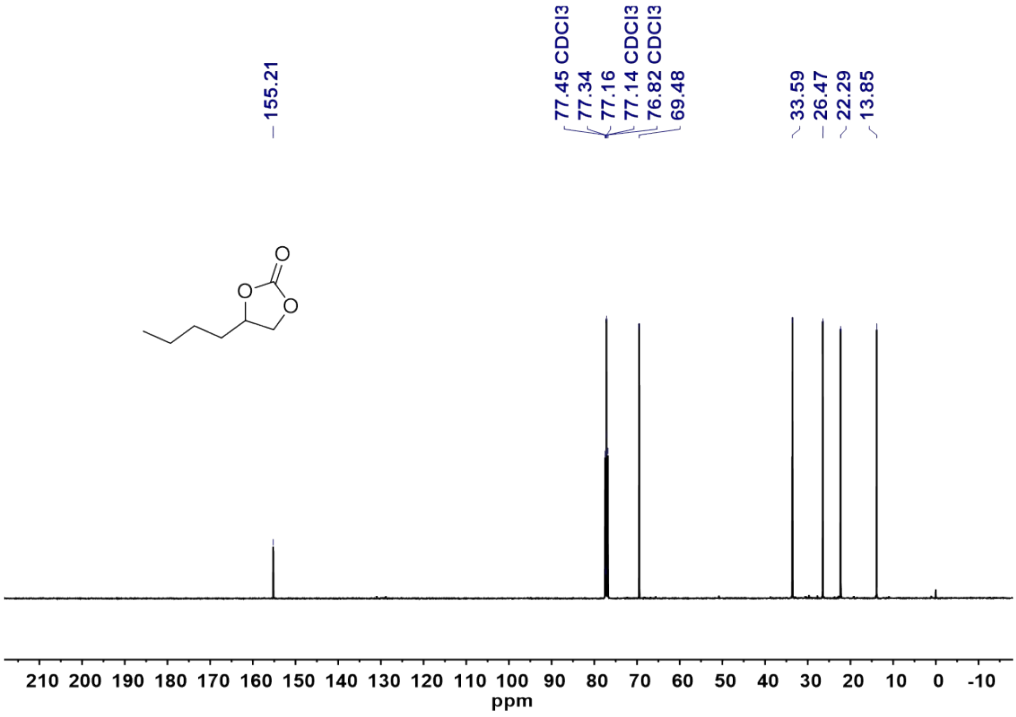

Figure S28. ^{13}C NMR spectrum ($CDCl_3$, 400 MHz) of 4-butyl-1,3-dioxane-2-one (obtained from crude reaction mass)

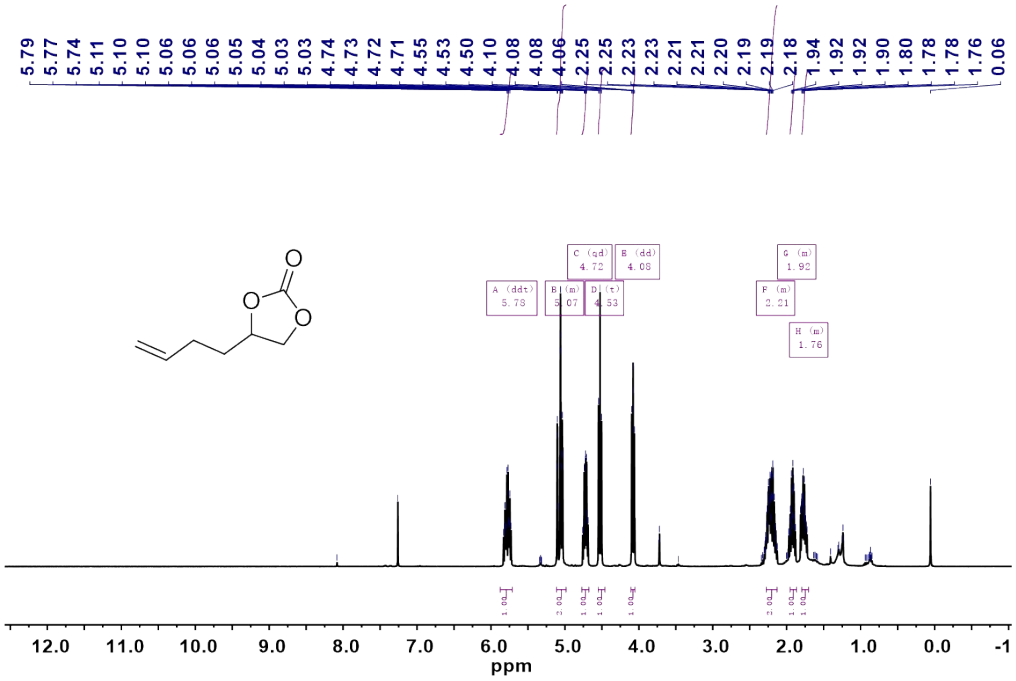

Figure S29. ^{1}H NMR spectrum ($CDCl_3$, 400 MHz) of cyclic carbonate 4-(but-3-en-1-yl)-1,3-dioxolan-2-one (obtained from crude reaction mass)

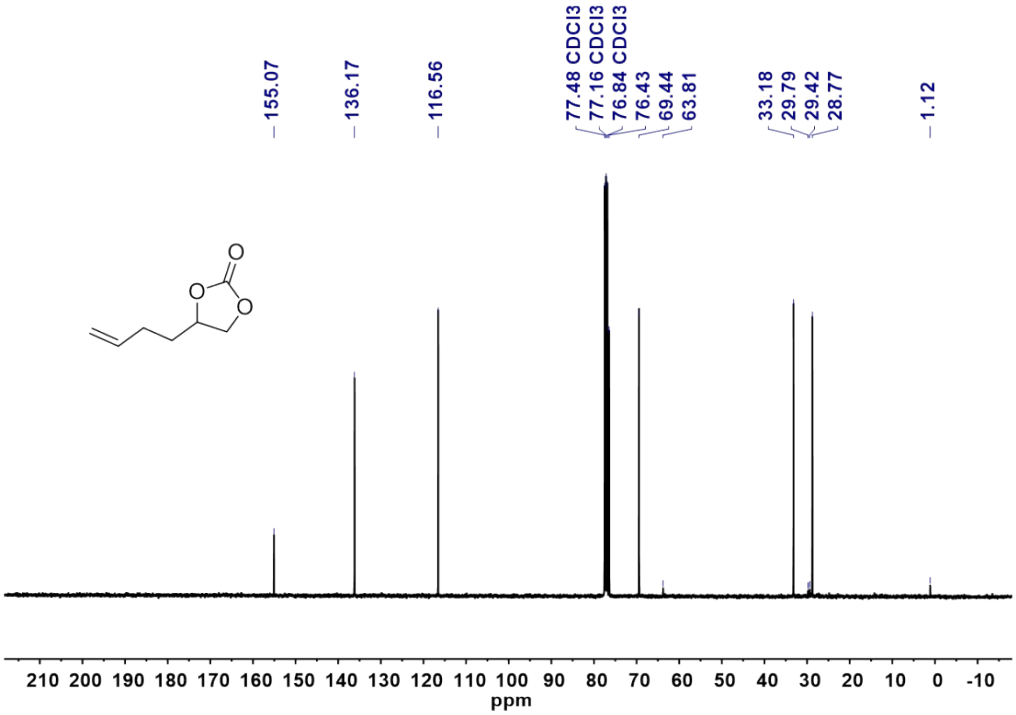

Figure S30. ^{13}C NMR spectrum ($CDCl_3$, 400 MHz) of 4-(but-3-en-1-yl)-1,3-dioxolan-2-one (obtained from crude reaction mass)

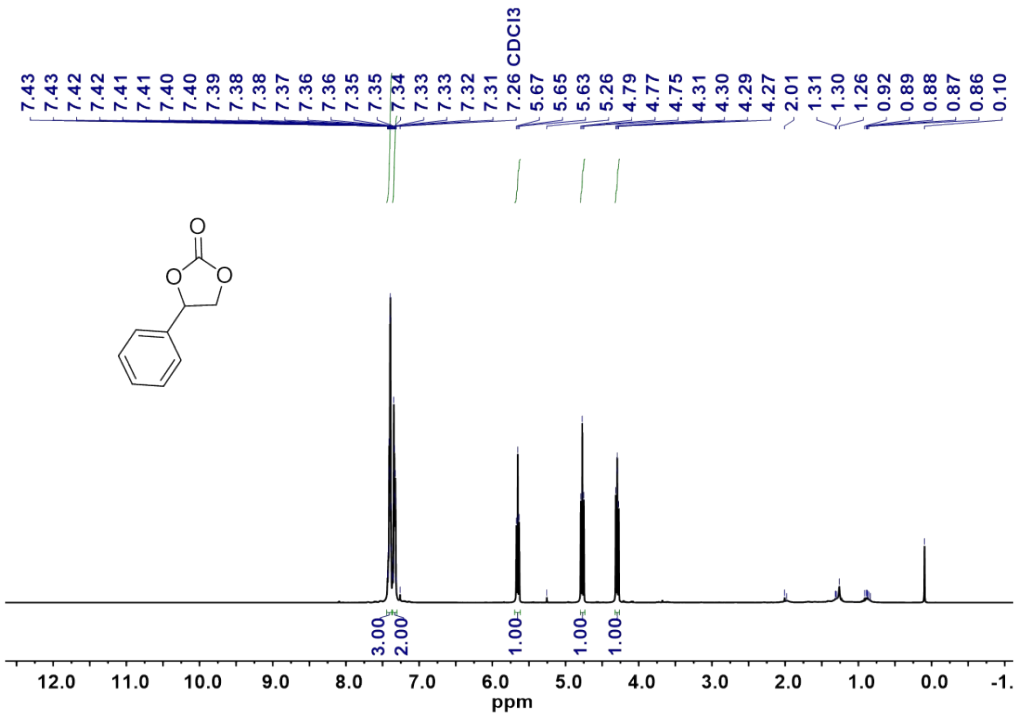

Figure S31. ^{1}H NMR spectrum ($CDCl_3$, 400 MHz) of 4-phenyl-1,3-dioxolan-2-one (obtained from crude reaction mass)

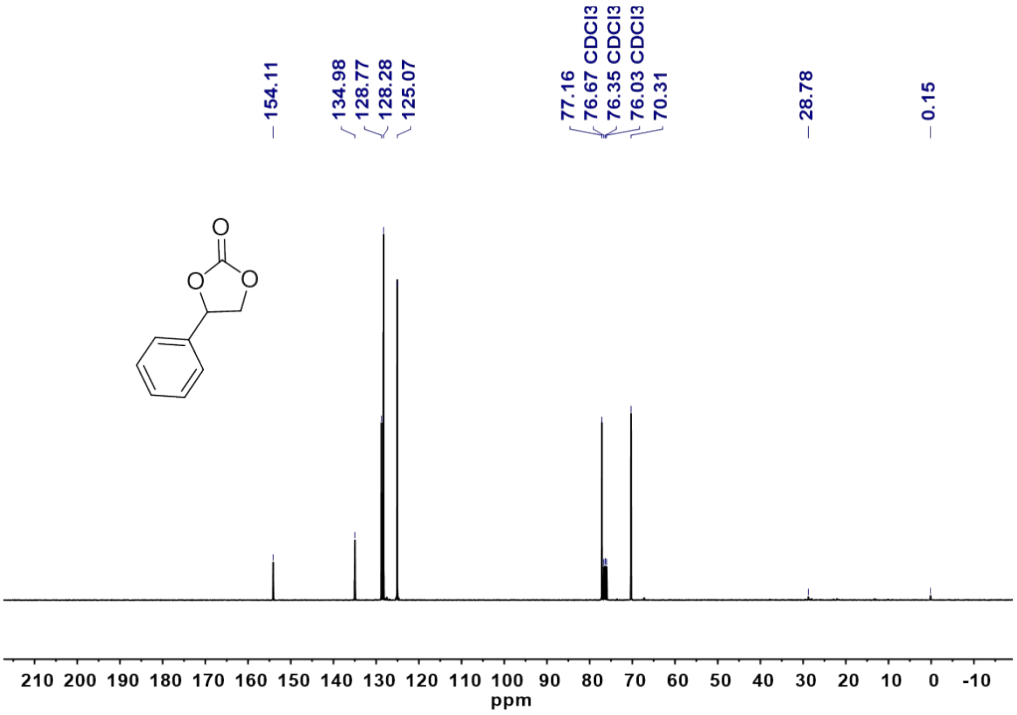

Figure S32. ^{13}C NMR spectrum ($CDCl_3$, 400 MHz) of 4-phenyl-1,3-dioxolan-2-one (obtained from crude reaction mass)

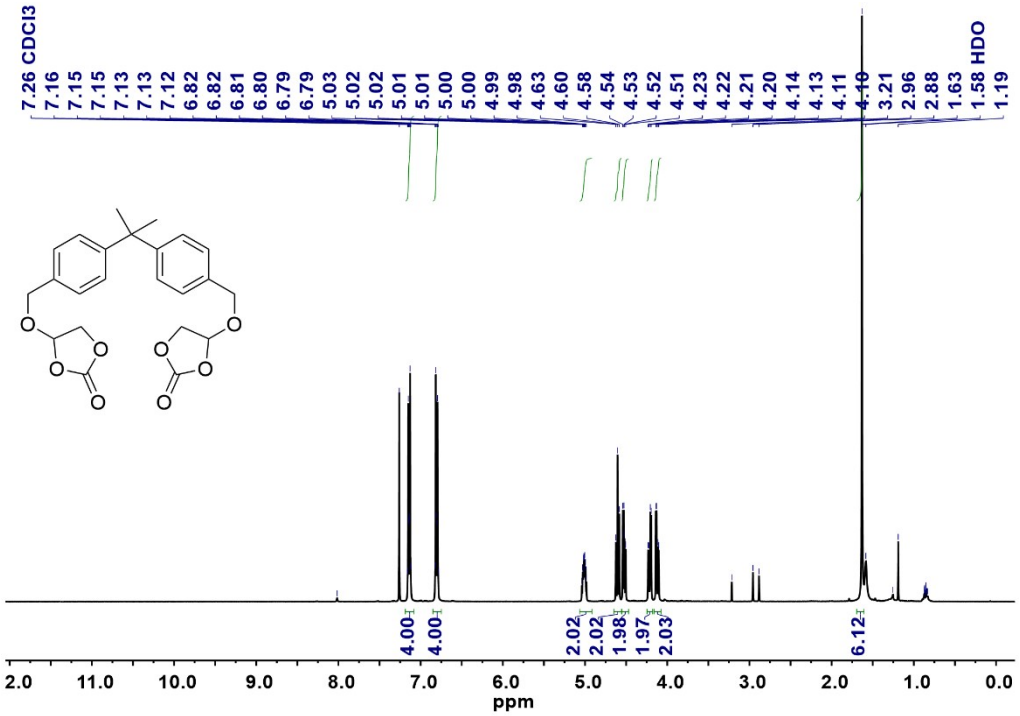

Figure S33. ^{1}H NMR spectrum ($CDCl_3$, 400 MHz) of 4,4'-(((Propane-2,2-diylbis(4,1-phenylene))bis(oxy)bis(methylene))bis(1,3-dioxolan-2-one) (obtained from crude reaction mass)

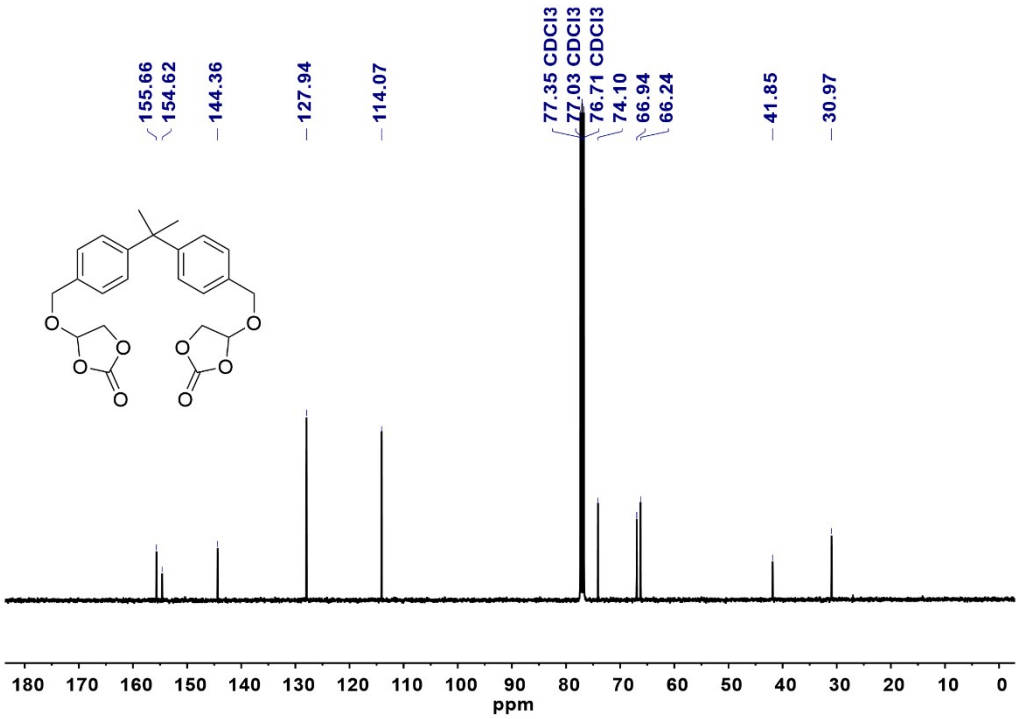

Figure S34. ^{13}C NMR spectrum ($CDCl_3$, 400 MHz) of 4,4'-(((Propane-2,2-diylbis(4,1-phenylene))bis(oxy)bis(methylene))bis(1,3-dioxolan-2-one) (obtained from crude reaction mass)

6. Copies and analysis of the ^{1}H NMR spectra of crude products (reaction mixture) of the CCE reactions

The CCE reaction mixture was cooled in ice before it was sampled for ^{1}H NMR measurements. The crude mixture of cyclic carbonate products was sampled of W_m mg, and there were W_i mg of internal standard 1,3,5-Trimethoxybenzene was added. Using 0.5 mL $CDCl_3$ to dissolve the mixture for ^{1}H NMR measurements. The integral values (I) of epoxides, cyclic carbonates and 1,3,5-Trimethoxybenzene (6.044 ppm) in ^{1}H NMR spectra were observed as I_e, I_c, and I_i. The molecular weights of cyclic carbonates are $M_{w,c}$, and 1,3,5-Trimethoxybenzene is $M_{w,i}$ (168.19 g/mol). The conversion (Conv.) and the selectivity were calculated from equation S1 (**eq. S1**) and equation S2 (**eq. S2**), respectively[1].

$$Conversion\ (\%) = \frac{I_c}{I_c + I_e}\ (eq.S1)$$

$$Selectivity\ of\ cyclic\ carbonate\ (\%) = \frac{3 \times W_i \times I_c \times M_{w,c}}{M_{w,i} \times I_i \times W_m \times Conv.}\ (eq.S2)$$

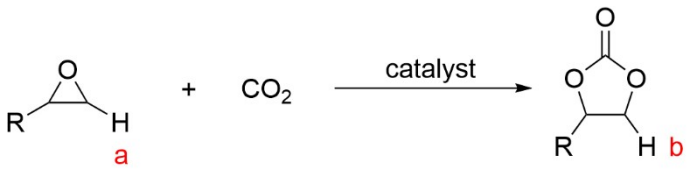

Scheme S1. Cycloadditions of CO_2 into epoxides for cyclic carbonates

Table S1. Chemical Shifts (δ, ppm, $CDCl_3$) for the epoxides (δ_a) and corresponding carbonate products (δ_b)

Entry	Epoxides	δ_a [ppm]	δ_b [ppm]
1	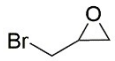	2.93	4.58
2	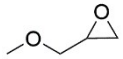	2.79	4.48
3	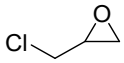	2.84	4.58
4	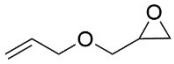	2.78	4.47
5	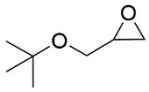	2.76	4.45
6	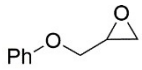	2.92	4.52
7	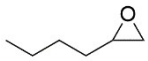	2.70	4.51
8	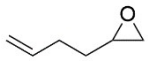	2.74	4.51

9	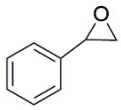	3.14	4.80
10	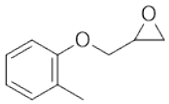	2.99	4.61
11	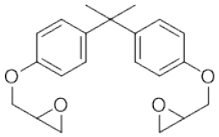	3.34	5.01

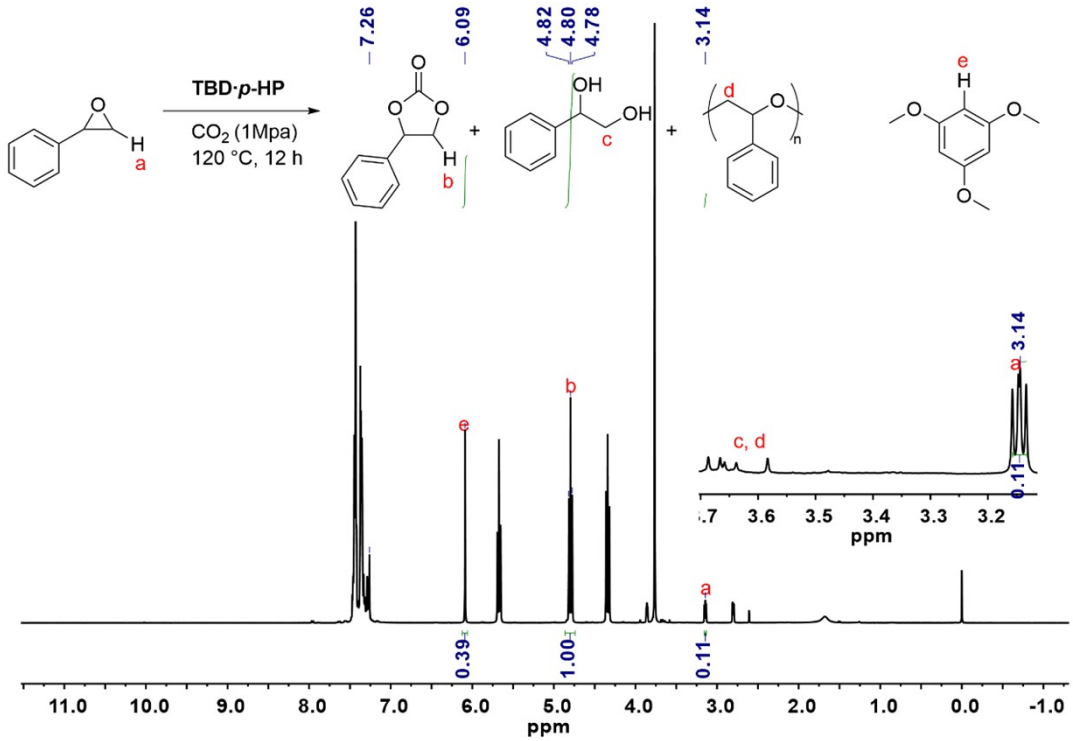

Figure S35. ^{1}H NMR Spectrum of crude CCE reaction mixture of styrene oxide (400 MHz, $CDCl_3$). Styrene oxide (10 mmol), **TBD·*p*-HP** (0.5 mol%), CO_2 (1 MPa), 24 h, 40.9 mg crude mixture, 4.5 mg 1,3,5-trimethoxybenzene (Table 3, entry 9). Conversion,90%; selectivity, 92%.

In the ^{1}H NMR spectrum (Figure S36) of crude styrene carbonate (Table 3, entry 9), W_c = 40.9 mg, W_i =4.5 mg, I_e = 0.11, I_c = 1, and I_i = 0.39. The conversion and the selectivity were calculated as:

$$Conversion\ (\%) = \frac{I_c}{I_c + I_e} = \frac{1}{1 + 0.11} = 90\%$$

$$Selectivity\ of\ cyclic\ carbonate\ (\%) = \frac{3 \times W_i \times I_c \times M_{w,c}}{M_{w,i} \times I_i \times W_m \times Conv.} = \frac{3 \times 4.51 \times 1 \times 164.16}{168.19 \times 0.39 \times 40.92 \times 0.90} = 92\%$$

In the ^{1}H NMR spectrum (Figure S35) of crude styrene carbonate (Table 3, entry 9), there were also some peaks of diol [4] by-product and polyether [5–7] by-product at 3.3–3.8 ppm were observed, and their presence led to the moderated selectivities of CCE reactions. Since the ion pair catalysts will partially decompose into the original organic base, the weakly basic but strongly nucleophilic bases (such as TBD) were able to directly attack the epoxides for diol (with H_2O) or polyether (with next epoxide) by-products due to the poor nucleofugality [8]. Using weakly nucleophilic phosphazene bases [9,10] was useful in improving the selectivity, but the unreacted phosphazene was also a good catalyst for polyether synthesis [11]. The generated phenolates were also found to nucleophilically attack the epoxide under low CO_2 pressure (≤ 1.0 MPa) [12] for diol and polyether, and it was suggesting that higher pressure of CO_2 (≥ 1.0 MPa) was probably improving the selectivity of pyridine-based halide-free catalysts.

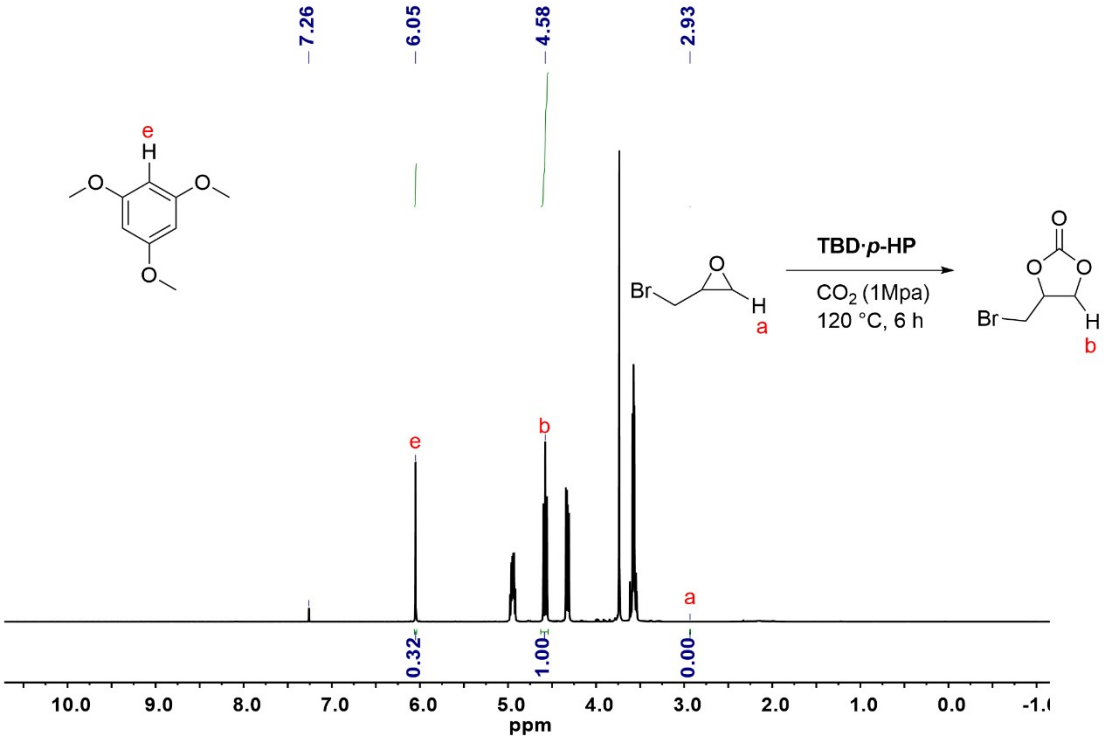

Figure S36. ^{1}H NMR Spectrum of crude CCE reaction mixture of 1-bromo-2,3-epoxypropane (400 MHz, $CDCl_3$). 1-Bromo-2,3-epoxypropane (10 mmol), **TBD·*p*-HP** (0.5 mol%), CO_2 (1 MPa), 6 h; 32.6 mg crude mixture, 3.2 mg 1,3,5-trimethoxybenzene (Table 3, entry 1). Conversion, >99%; selectivity, >99%.

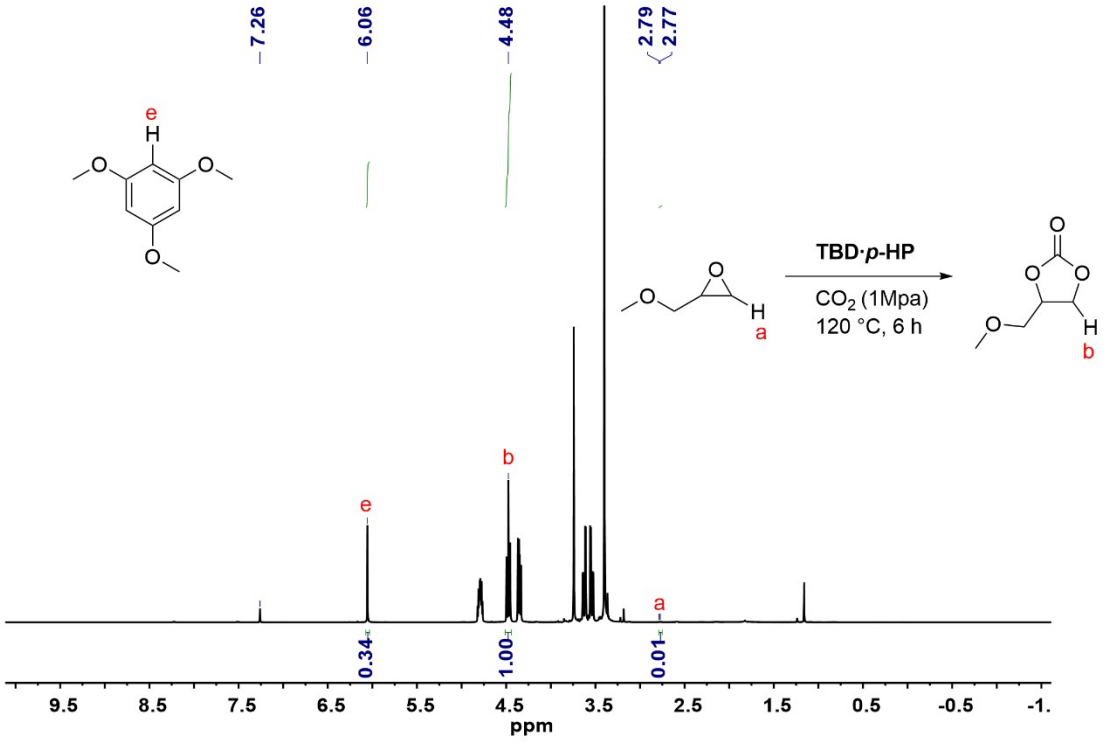

Figure S37. ^{1}H NMR Spectrum of crude CCE reaction mixture of glycidyl phenyl ether (400 MHz, $CDCl_3$). Glycidyl phenyl ether (10 mmol), **TBD·*P*-HP** (0.5 mol%), CO_2 (1 MPa), 24 h; 42.3 mg crude mixture, 6.0 mg 1,3,5-trimethoxybenzene (Table 3, entry 2). Conversion, 99%; selectivity, >99%.

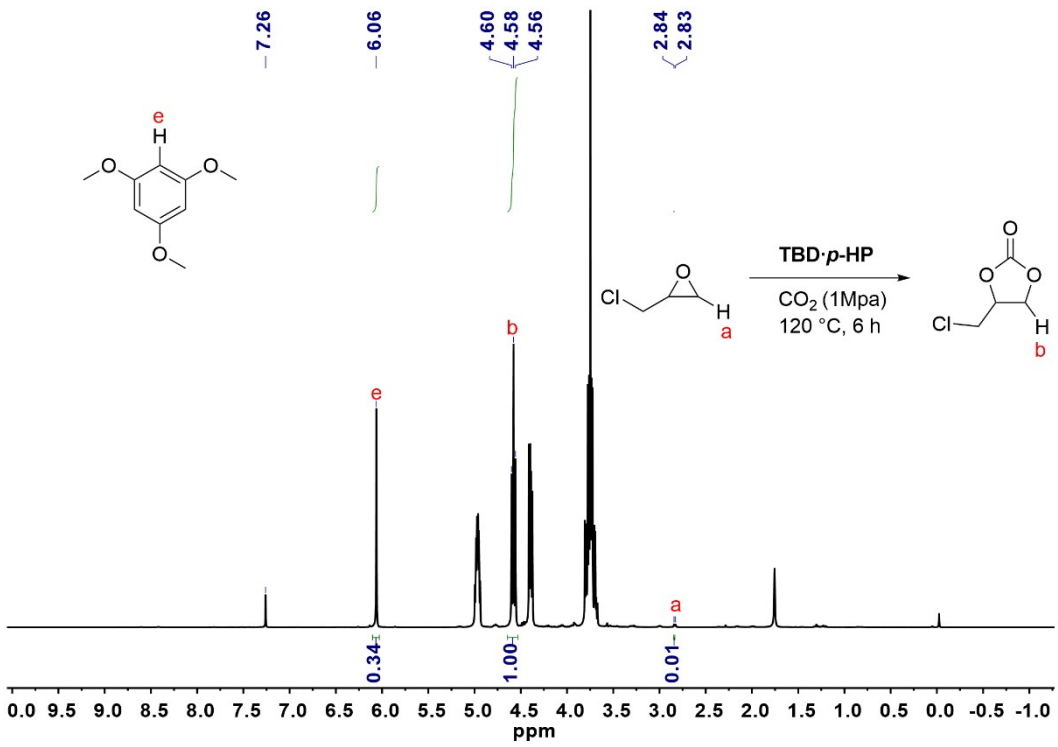

Figure S38. ^{1}H NMR Spectrum of crude CCE reaction mixture of epichlorohydrin (400 MHz, $CDCl_3$). Epichlorohydrin (10 mmol), **TBD·*P*-HP** (0.5 mol%), CO_2 (1 MPa), 6 h; 38.7 mg crude mixture, 5.2 mg 1,3,5-trimethoxybenzene (Table 3, entry 3). Conversion, >99%; selectivity, >99%.

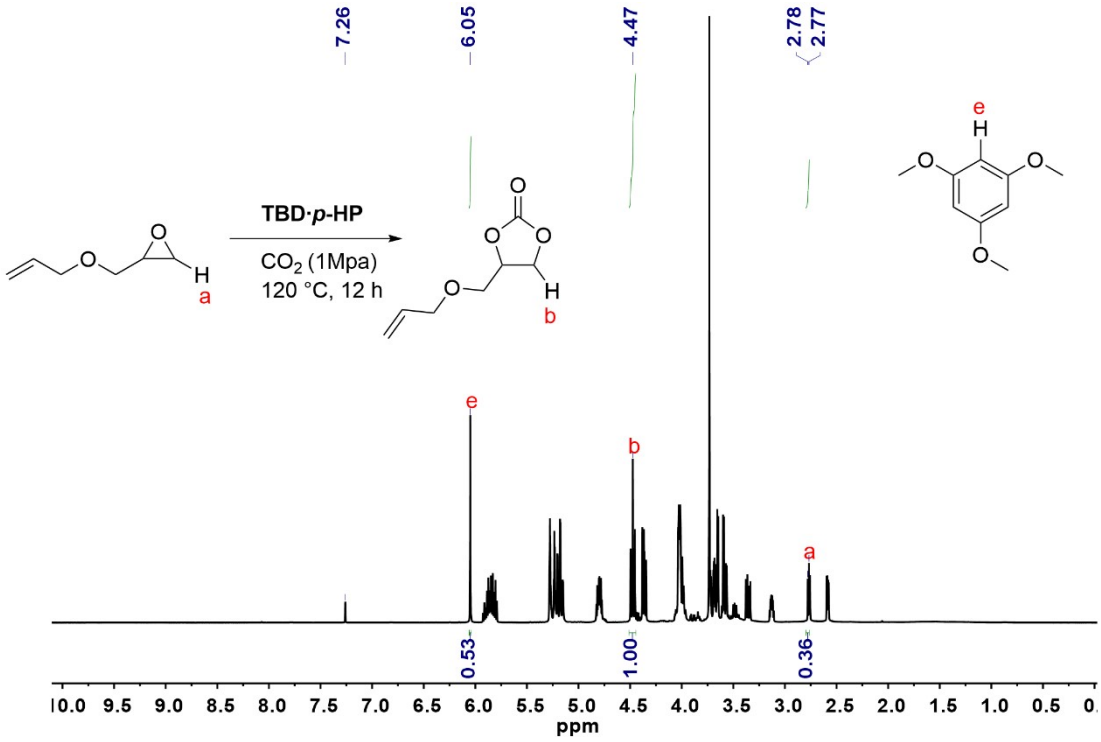

Figure S39. ^{1}H NMR Spectrum of crude CCE reaction mixture of allyl glycidyl ether (400 MHz, $CDCl_3$). Allyl glycidyl ether (10 mmol), **TBD·*P*-HP** (0.5 mol%), CO_2 (1 MPa), 12 h; 40.2 mg crude

mixture, 5.2 mg 1,3,5-trimethoxybenzene. Conversion, 69%; selectivity, 99%.

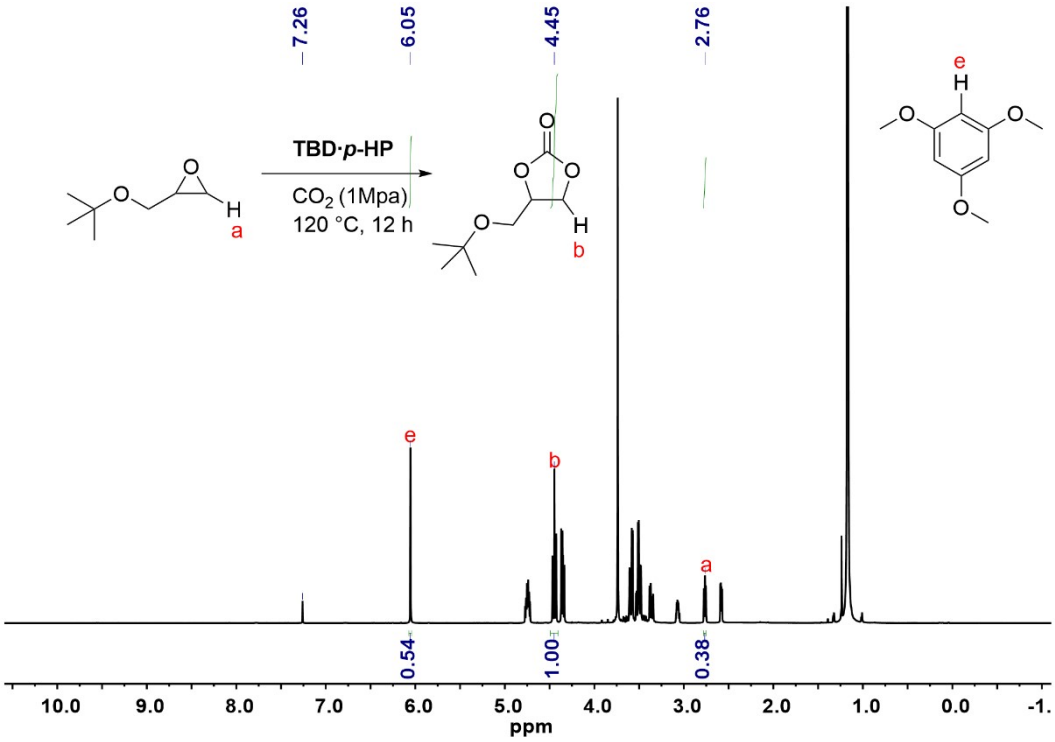

Figure S40. ^{1}H NMR Spectrum of crude CCE reaction mixture of *tert*-butyl glycidyl ether (400 MHz, $CDCl_3$). *tert*-Butyl glycidyl ether (10 mmol), **TBD·*P*-HP** (0.5 mol%), CO_2 (1 MPa), 12 h; 38.7 mg crude mixture, 4.4 mg 1,3,5-trimethoxybenzene. Conversion, 66%; selectivity, 99%.

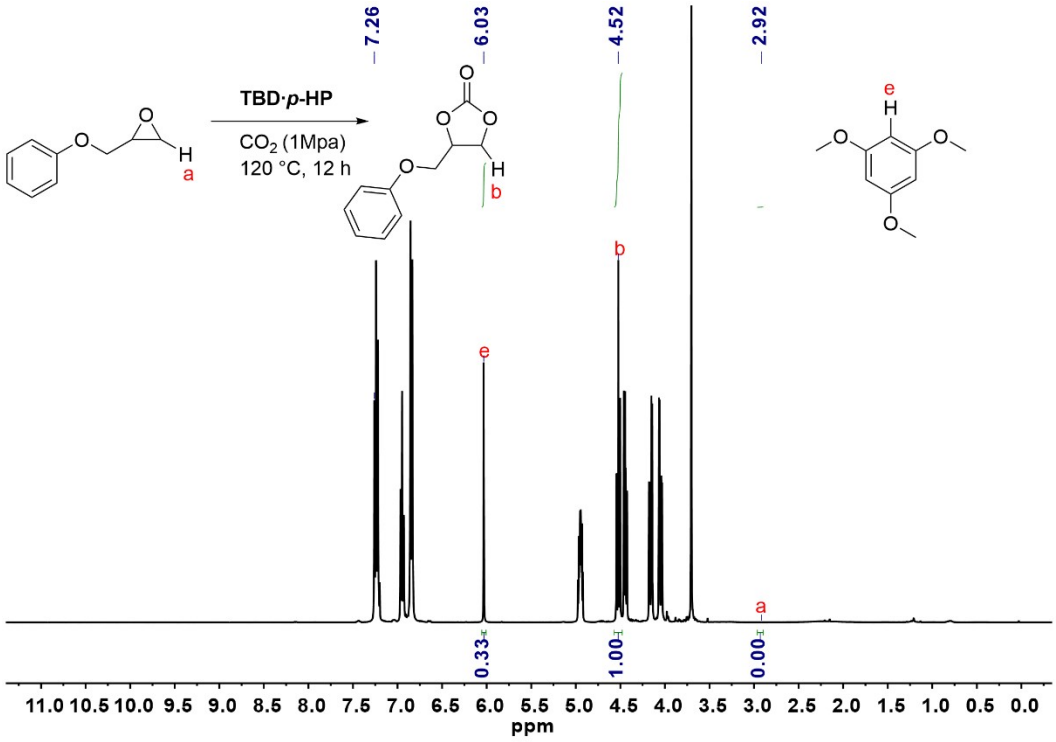

Figure S41. ^{1}H NMR Spectrum of crude CCE reaction mixture of glycidyl phenyl ether (400 MHz, $CDCl_3$). Glycidyl phenyl ether (10 mmol), **TBD·*P*-HP** (0.5 mol%), CO_2 (1 MPa), 24 h; 41.6 mg crude mixture, 3.9 mg 1,3,5-trimethoxybenzene (Table 3, entry 6). Conversion, >99%; selectivity, >99%.

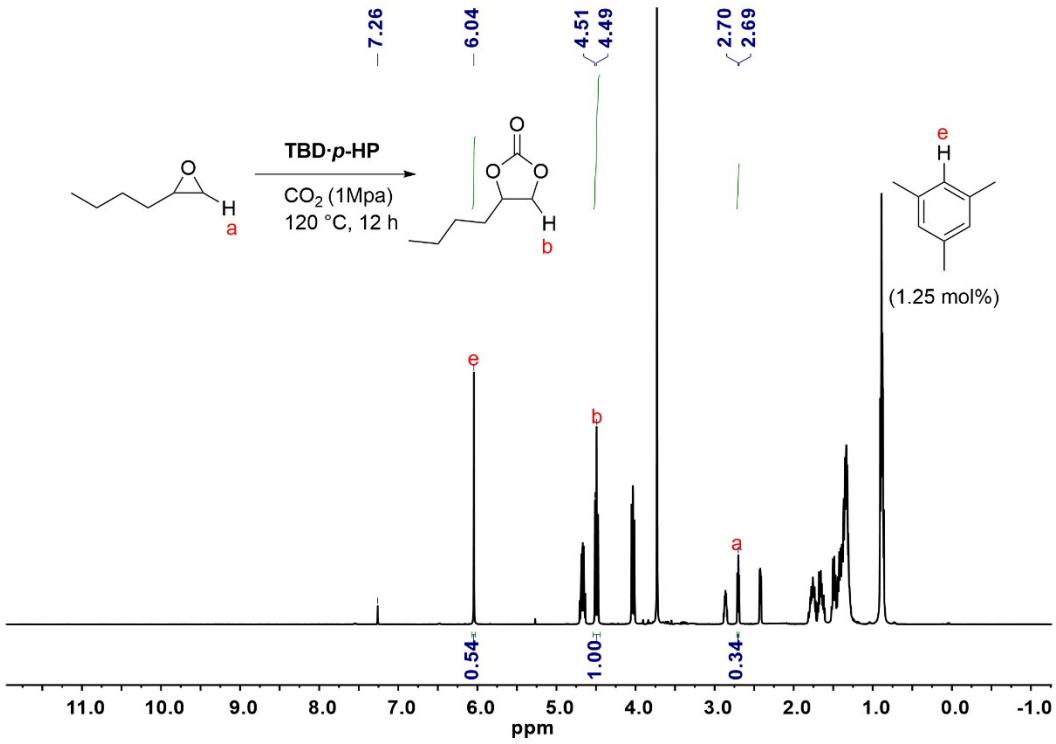

Figure S42. ^{1}H NMR Spectrum of crude CCE reaction mixture of 1,2-epoxyhexane (400 MHz, $CDCl_3$). 1,2-Epoxyhexane (10 mmol), **TBD·*P*-HP** (0.5 mol%), CO_2 (1 MPa), 12 h; 44.9 mg crude mixture, 6.3 mg 1,3,5-trimethoxybenzene. Conversion, 69%; selectivity, 99%.

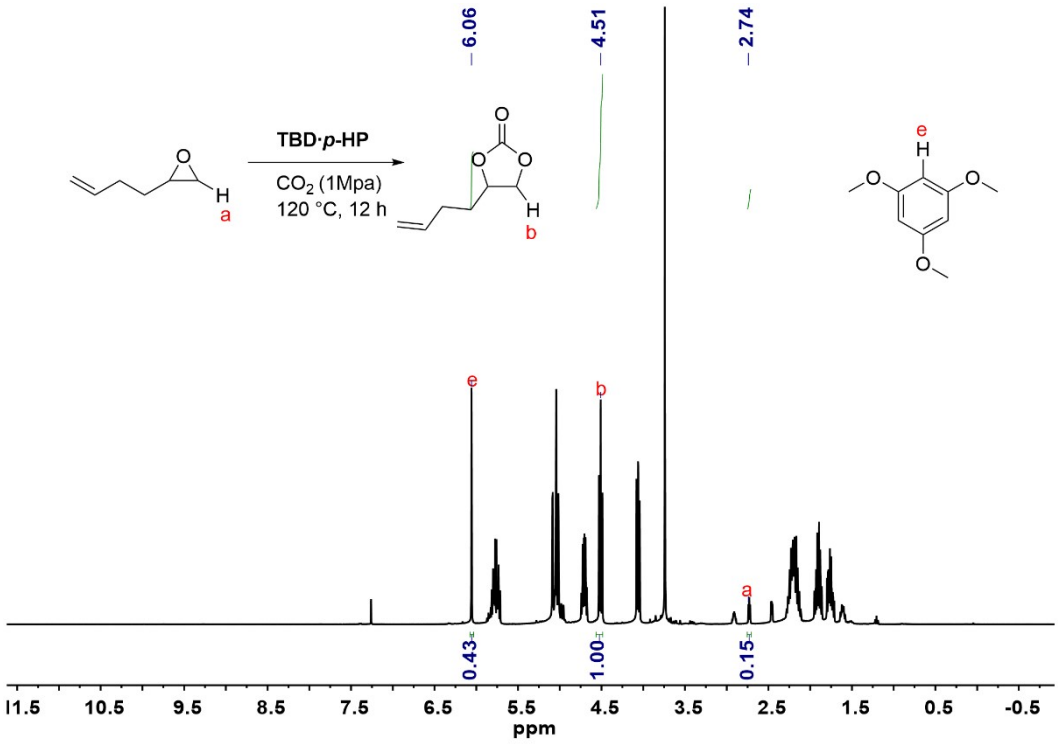

Figure S43. ^{1}H NMR Spectrum of crude CCE reaction mixture of 2-(but-3-en-1-yl)oxirane (400 MHz, $CDCl_3$). 2-(But-3-en-1-yl)oxirane (10 mmol), **TBD·*P*-HP** (0.5 mol%), CO_2 (1 MPa), 24 h; 37.8 mg crude mixture,5.4 mg 1,3,5-trimethoxybenzene(Table 3, entry 8). Conversion, 87%; selectivity, 98%.

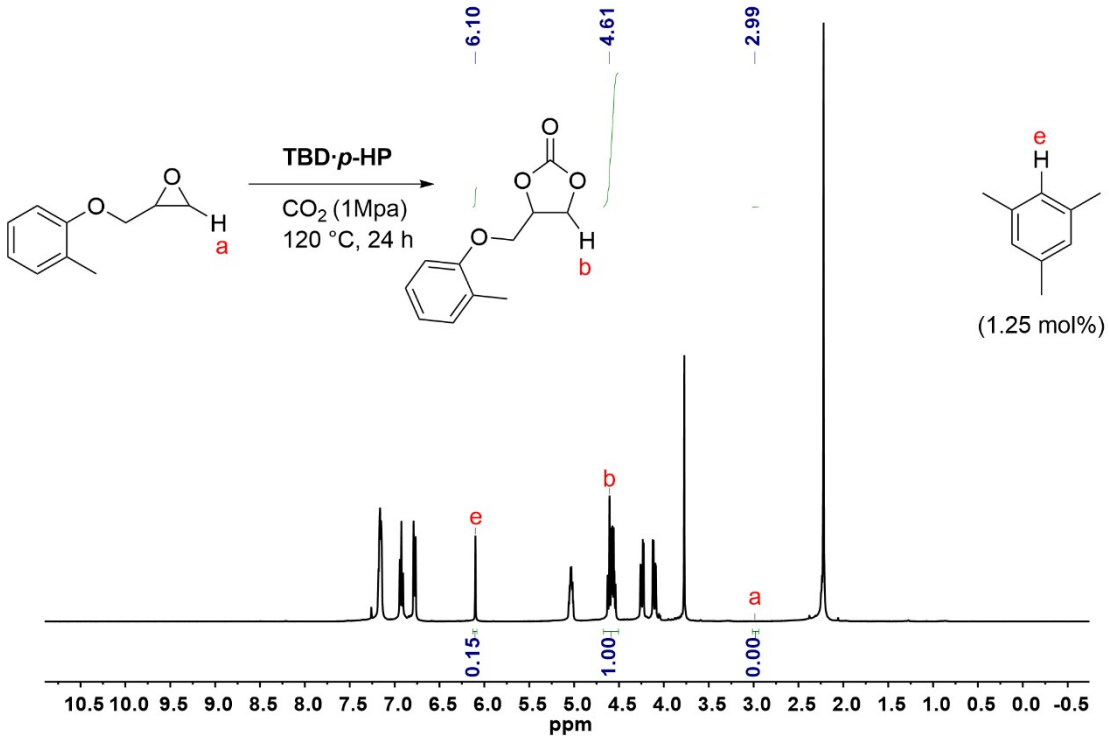

Figure S44. ^{1}H NMR Spectrum of crude CCE reaction mixture of 2-((*o*-tolyloxy)methyl)oxirane (400 MHz, $CDCl_3$). 2-((*o*-Tolyloxy)methyl)oxirane (10 mmol), **TBD·*P*-HP** (0.5 mol%), CO_2 (1 MPa), 24 h; 46.7 mg crude mixture, 1.8 mg 1,3,5-trimethoxybenzene(Table 3, entry 10). Conversion, >99%; selectivity, >99%.

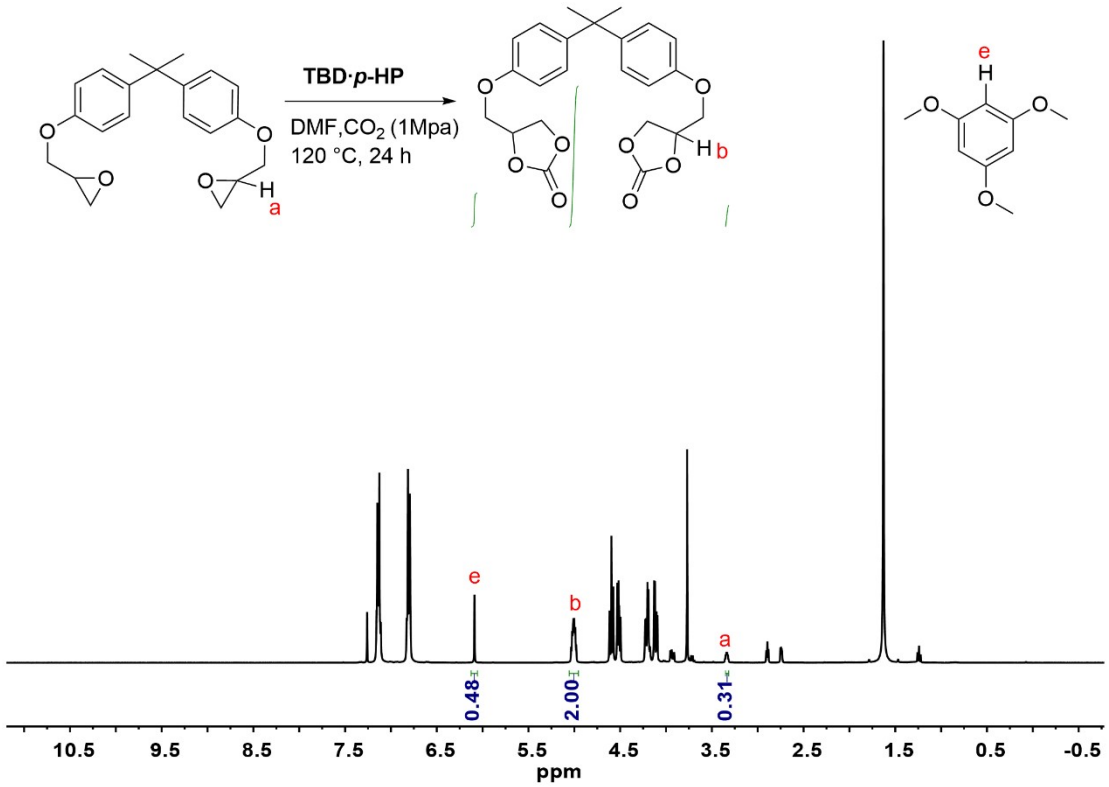

Figure S45. ^{1}H NMR Spectrum of crude CCE reaction mixture of 2-((*o*-tolyloxy)methyl)oxirane

(400 MHz, $CDCl_3$). 2,2'-(((propane-2,2-diylbis(4,1-phenylene))bis(oxy))bis(methylene))bis(oxirane) (10 mmol), **TBD·*P*-HP** (0.5 mol%), CO_2 (1 MPa),24 h; 90.2 mg crude mixture, 7.8 mg 1,3,5-trimethoxybenzene (Table 3, entry 11). Conversion, 87%; selectivity, >99%.

5. Thermogravimetric analysis of catalysts (Figure S46)

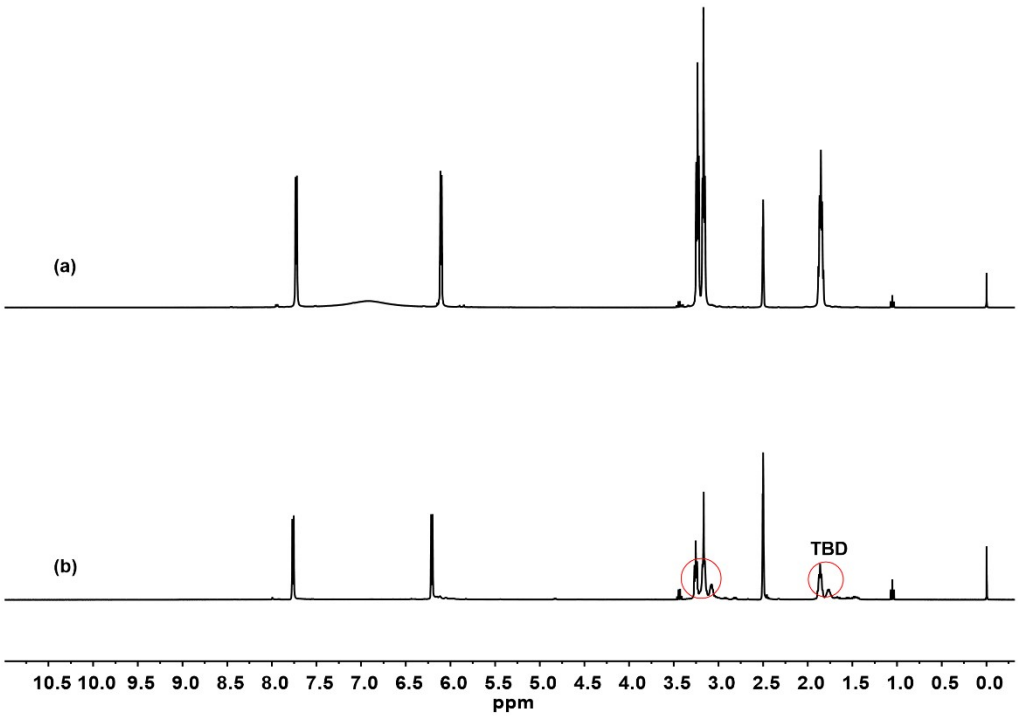

Figure S46. ^{1}H spectra (DMSO-d_6) of **TBD·*p*-HP**, (a), Pure **TBD·*p*-HP**, (b), 1 mmol of **TBD·*p*-HP** , 120 °C, 24 h.

6. Thermogravimetric analysis of catalysts (Figure S47 – Figure S48)

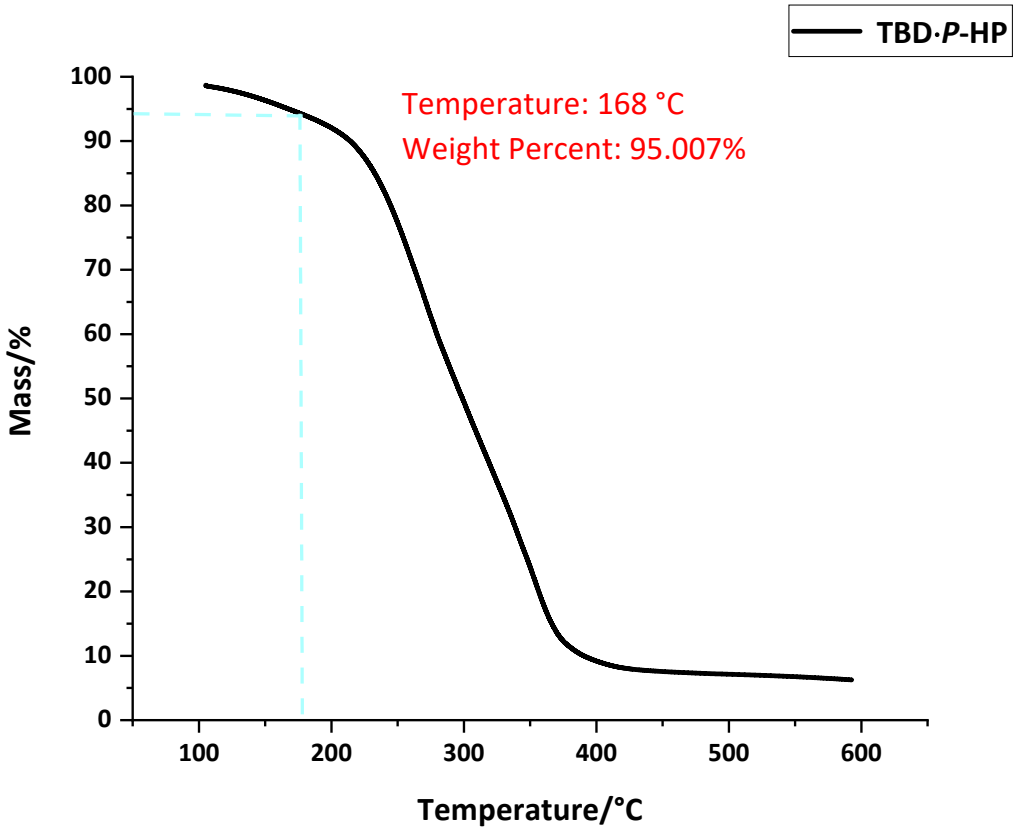

Figure S47. Thermogravimetric analysis of catalyst **TBD·*p*-HP**

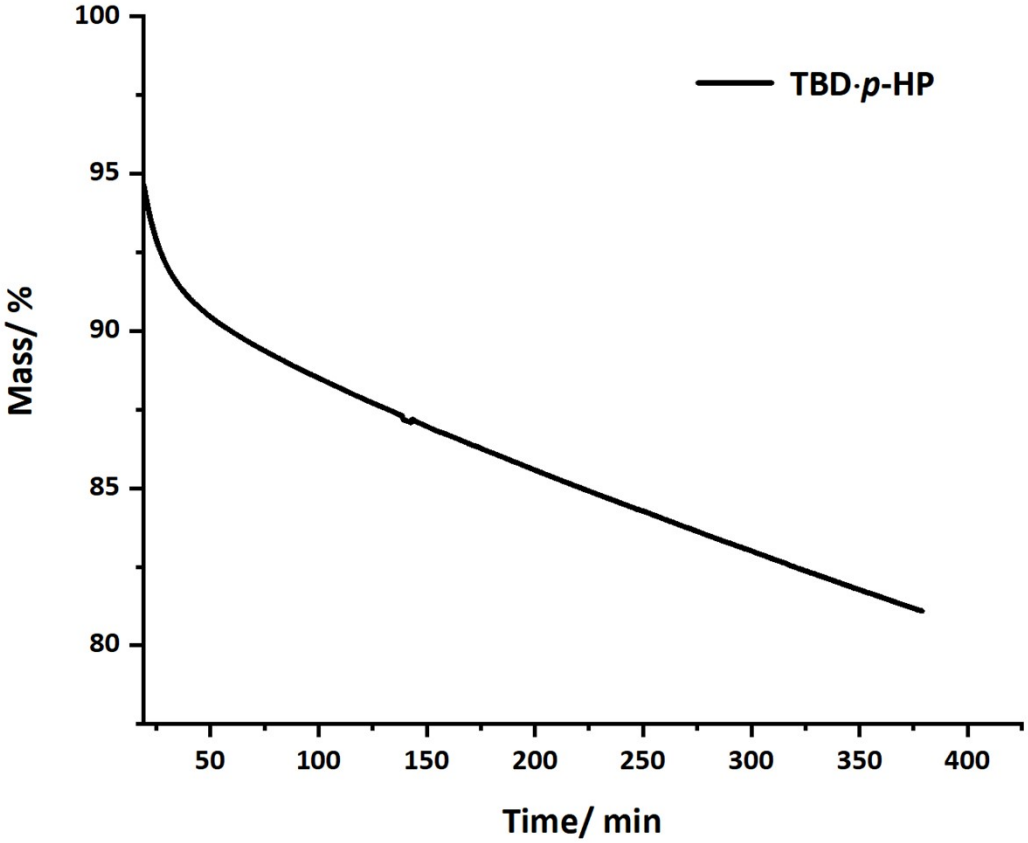

Figure S48**.** The TGA plot of **TBD·*p*-HP** at a constant temperature of 120 °C.

References

1. J.X. Xu, A.M. Xian, Z.J. Li, J.J. Liu, Z.H. Zhang, R. Yan, L.Y. Gao, B. Liu, L.L. Zhao, K. Guo. A Strained Ion Pair Permits Carbon Dioxide Fixation at Atmospheric Pressure by C-H H-Bonding Organocatalysis. J. Org. Chem., 2021, 86: 3422–3432.
2. A. Rostami, M. Mahmoodabadi, A.H. Ebrahimi, H. Khosravi, A. Al-Harrasi. An Electrostatically Enhanced Phenol as a Simple and Efficient Bifunctional Organocatalyst for Carbon Dioxide Fixation. ChemSusChem, 2018, 11: 4262–4268.
3. H.Y. Tong, Y.Y. Qu, Z.J. Li, J. He, X. Zou, Y. Zhou, T. Duan, B. Liu, J. Sun, K. Guo. Halide-free pyridinium saccharinate binary organocatalyst for the cycloaddition of CO_2 into epoxides[J]. Chem. Eng. J., 2022, 444: 135478.
4. B. Liu, H. Yu, Z.J. Li, J. He, Y.Z. Hu, X. Zou, L.L. Lu, S.J Cao, C.L. Ma, K. Guo. Halide-free squaramide–phenolate organocatalyst for the cycloaddition of CO_2 into epoxides. J. Environ. Chem. Eng. 2023,11: 110886.
5. C. Robert, T. Ohkawara, K. Nozaki. Manganese-Corrole Complexes as Versatile Catalysts for the Ring-Opening Homo- and Co-Polymerization of Epoxide. Chem. Eur. J. 2014**,** 20: 4789-4795.
6. C.L. Bentley, T. Song, B.J. Pedretti, M.J. Lubben, N.A. Lynd, J.F. Brennecke. Effects of Poly(glycidyl ether) Structure and Ether Oxygen Placement on CO_2 Solubility. J. Chem. Eng. Data. 2021**,** 66: 2832–2843.
7. J. Hilf, P. Schulze, H. Frey. CO_2-Based Non-ionic Surfactants: Solvent-Free Synthesis of Poly(ethylene glycol)-block-Poly(propylene carbonate) Block

Copolymers. Macromol. Chem. Phys. 2013, 214: 2848–2855.

8. M. Baidya, H. Mayr. Nucleophilicities and carbon basicities of DBU and DBN. Chem. Commun., 2008, 15: 1792–1794.

9. Y. Kondo. Phosphazene: Preparation, Reaction and Catalytic Role. In Superbases for Organic Synthesis, 2009; 145–185.

10. L. Harwood, T. Ishikawa. Organic Superbases: The Concept at a Glance. Synlett 2013, 24: 2507–2509.

11. S. Boileau, N. Illy. Activation in anionic polymerization: Why phosphazene bases are very exciting promoters. Prog. Polym. Sci., 2011, 36: 1132–1151.

12. X.Y. Luo, Y. Guo, F. Ding, H.Q. Zhao, G.K. Cui, H.R. Li, C.M. Wang. Significant improvements in CO_2 capture by pyridine-containing anion-functionalized ionic liquids through multiple-site cooperative interactions. Angew. Chem. Int. Ed. Engl., 2014, 53: 7053–7057.